Table 2. Strabismus and the Ala20 polymorphism of *PMX2B* gene

Sample	Strabismus	*n*	Genotype counts[a]					*P*-value[b]
			0/0	0/−15	−15/−15	0/−21	0/+6	
Control	Constant exotropia	2	2	0	0	0	0	1.000
	No strabismus	515	472	33	3	6	1	
Schizophrenia	Constant exotropia	24	17	6	0	0	1	0.029
	No strabismus	300	266	32	0	1	1	
Total	Constant exotropia	41	19	6	0	0	1	0.017
	No strabismus	815	738	65	3	7	2	

[a]0 indicates the wild type allele, and − or + denotes the variant alleles with the indicated number of deletions (−) or insertions (+) of Ala20-coding nucleotides.
[b]*P*-value for association was calculated by Fisher's exact test.

Table 3. Schizophrenia and the Ala20 polymorphism of *PMX2B* gene

Subjects	*n*	Genotype counts (%)[a]					*P*-value[b]
		0/0	0/−15	−15/−15	0/−21	0/+6	
Total schizophrenia	324	283 (87)	38 (12)	0 (0)	1 (0.3)	2 (0.6)	0.012
Without strabismus	300	266 (87)	32 (11)	0 (0)	1 (0.3)	1 (0.3)	0.076
With constant exotropia	24	17 (71)	6 (25)	0 (0)	0 (0)	1 (4.2)	0.004
Controls[c]	515	472 (92)	33 (6.4)	3 (0.6)	6 (1.2)	1 (0.2)	

[a]0 indicates the normal allele, and − or + denotes the variant alleles with the indicated number of deletions (−) or insertions (+) of the Ala20-coding nucleotides.
[b]*P*-value for association was calculated by Fisher's exact test.
[c]Subjects who had strabismus were excluded.

samples. Information on primer sequences used in this study is available on request.

Genotyping of *PMX2B* polymorphisms

The genomic region encoding the 20 alanine (Ala20) tract was amplified using fluorescently labeled forward primer (5′-AACCCGGCAAGGGCGGCGCAGCA, 3′ end at nt c.726) and reverse primer (5′-GAAGGGACCCCCAAGCGAAT, 3′ end at nt c.854), rTaq polymerase (Takara, Tokyo, Japan) and MasterAmp K buffer (Epicentre Technologies, Madison, WI). To avoid artefactual −3 base shifts seen in templates with c.762C, we added 0.2 mM of 7-deaza-2′-deoxyguanosine triphosphate (c^7dGTP) to PCR reaction mixtures (Fig. 5). PCR products were run on an ABI 3700 genetic analyzer and the resulting data analyzed using GeneScan and Genotyper software (Applied Biosystems, Foster City, CA). Genotypes of mutants were verified using both direct sequencing and subcloning of amplicons into a TA vector (Invitrogen, Carlsbad, CA) and sequencing. Sequencing was performed using a DYEnamic ET terminator cycle sequencing kit (Amersham Biosciences, Piscataway, NJ). TaqMan assay was used to type SNP markers (Applied Biosystems). The mouse Ala20 tract of *Pmx2b* was examined in 120 C57BL/6 mice, 120 C3H/He mice and 120 of the F1 progeny, using the forward primer (5′-AGGCGAACCCGGCAAGGGCGGT, 3′ end at nt c.657) and reverse primer (5′-GAAGGGCCCCCCAAGA GAATCT, 3′ end at c.789).

Constructs for luciferase assay

The coding region of *PMX2B* (accession no. NM_003924) was amplified using Human Brain Marathon-Ready cDNA as a template (Clontech, Palo Alto, CA), then cloned into pIRES-neo2 expression vector (Clontech). Altered Ala20 length constructs were prepared by swapping the Ala20 region with those amplified from mutant genomic DNA or using PCR-based techniques (40). The gene promoter for dopamine β-hydroxylase (*DBH*) (41) was amplified using a primer set designed from the genomic sequence (accession no. AC001227), then cloned into the pGL3-basic reporter vector (Promega, Madison, WI). Constructs lacking the entire Ala20 and Ala9 regions were generated using PCR-based techniques (40).

Transfection and luciferase assay

HepG2 cells were purchased from the Riken Cell Bank (Tsukuba, Japan). The plasmid mixture was prepared by combining 1.3 μg of construct DNA (pIRES-neo2-*PMX2B*:pGL3-basic-*DBH* promoter = 400 μg : 900 μg), 100 μg of pRL-TK as an internal control and 2.5 μl of LipofectAMINE2000 in 100 μl of OPTI-MEM (Invitrogen). Transfections were performed using Lipofect AMINE2000 (Invitrogen) according to the instructions of the manufacturer. Transcriptional assay was performed using the PicaGene Dual SeaPansy kit in accordance with the manufacturer's instructions (Toyo Ink, Tokyo, Japan). Luciferase activity was measured using a luminometer Lumat LB 9507 (EG&G Berthold, Bad Wildbad, Germany).

Statistical analyses

Phenotype–genotype association tests were assessed using the χ^2 test, or Fisher's exact test where appropriate. Linkage disequilibrium (LD) statistics were calculated using COCAPHASE (42) (http://www.hgmp.mrc.ac.uk/~fdudbrid/software/), and estimation

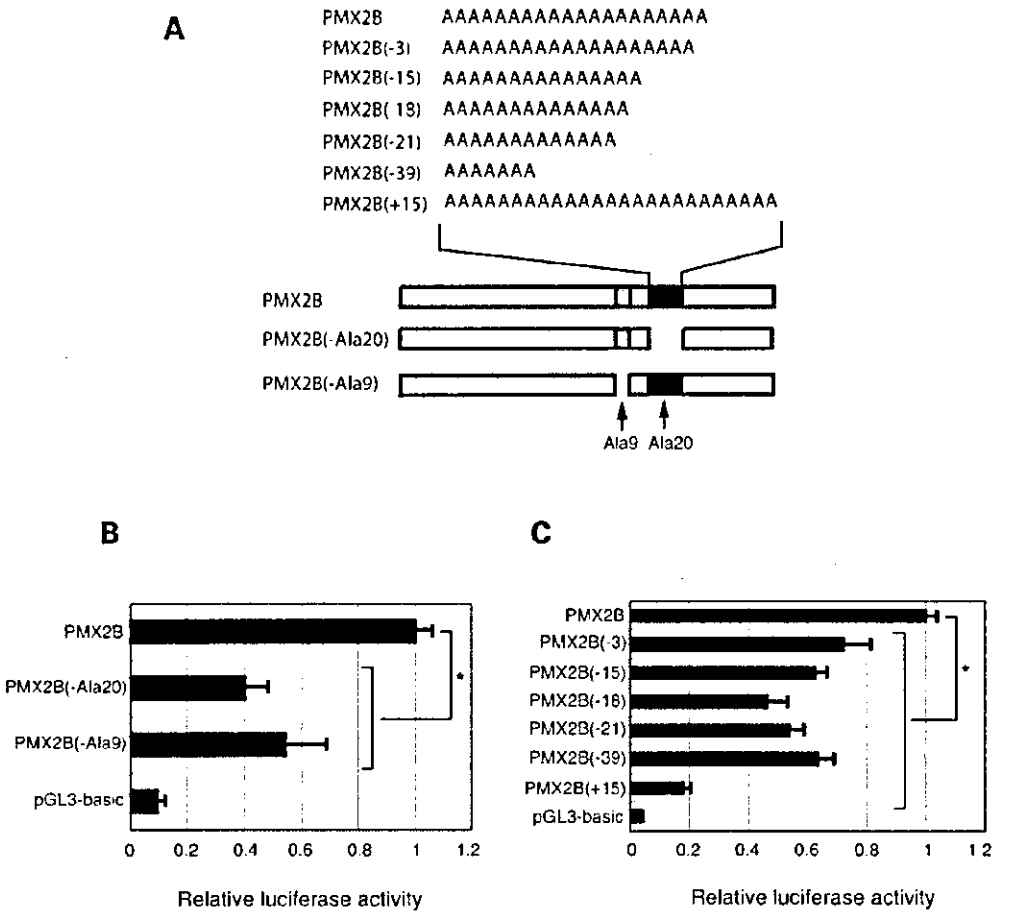

Figure 6. Functional consequences of *PMX2B* mutant alleles. Preparation of *PMX2B* deletion/insertion mutants is shown (**A**). A, alanine. Effects of Ala20 and Ala9 stretch deletions were examined under luciferase assay. Reporter constructs containing the *DBH* promoter were co-transfected into HepG2 cells with either normal *PMX2B* or deletion mutants. Luciferase activity of each construct was normalized by the internal control, pRL-TK. Activity of the normal *PMX2B* was defined as 1. Results shown represent means ± SEM for at least three separate transfections, each run in triplicate. pGL3-basic is a promotorless negative control vector. $^*P < 0.01$ by Tukey–Kramer multiple comparison test (**B**). Assay of Ala20 mutants was performed under the same conditions as in B (**C**). $^*P < 0.01$ by Tukey-Kramer test.

Table 4. Pairwise linkage disequlibrium estimations between polymorphisms in the *PMX2B* gene

Polymorphism	IVS1-385G>A (SNP1)	IVS1-115G>A (SNP2)	IVS2+101A>G (SNP3)	IVS2-404-405delAG (SNP4)	c.1618insT (SNP5)	c.2309G>A (SNP6)
SNP1	—	1.000	1.000	1.000	1.000	1.000
SNP2	1.000	—	1.000	1.000	1.000	1.000
SNP3	0.984	0.984	—	0.984	1.000	1.000
SNP4	0.984	0.984	0.968	—	1.000	1.000
SNP5	0.969	0.969	0.954	0.954	—	0.967
SNP6	0.86	0.858	0.846	0.846	0.831	—

Values above the diagonal show standardized D' in 200 unrelated subjects, calculated by using the COCAPHASE program. Values below the diagonal show r^2 (squared correlation coefficient).
The polymorphisms used in this linkage disequlibrium analysis (SNPs1–6) were those whose minor allele frequencies were more than 3% (also see Fig. 1).
The Ala20 stretch is located between SNP4 and SNP5.

of haplotype frequencies and assessment of Hardy–Weinberg equilibrium were performed using Arlequin software (http://lgb.unige.ch/arlequin/). Genotype data from 100 males and 100 females were used for LD and haplotype analyses. CLUSTALW (program for multiple alignments and tree-making; http://www.ddbj.nig.ac.jp/E-mail/clustalw-e.html) (43) and TreeView ver.1.6.6 (program for displaying phylogenies; http://taxonomy.zoology.gla.ac.uk/rod/treeview.html) (44) software

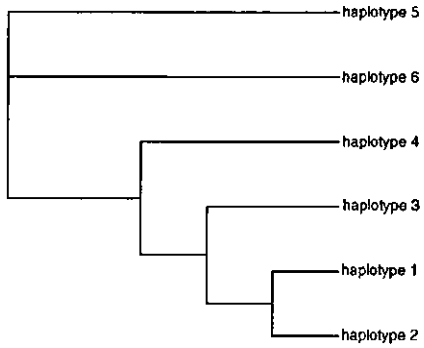

	SNP1	SNP2	SNP3	SNP4	Ala20	SNP5	SNP6	frequency
haplotype 1	A	A	G	D	1	I	A	0.0784
haplotype 2	A	A	G	D	2	I	A	0.1303
haplotype 3	G	G	A	I	1	D	A	0.0262
haplotype 4	G	G	A	I	1	D	G	0.6453
haplotype 5	G	G	A	I	2	D	G	0.0379
haplotype 6	G	G	A	I	3	D	G	0.0608

Figure 7. Phylogram of haplotypes in *PMX2B*. For nomenclature of SNPs 1–6, see Figure 1. For SNP4, 'D' indicates deletion and 'I' denotes insertion. For Ala20, allele 1 = c.762A, allele 2 = c.762C, allele 3 = 15-bp deletion. Six different haplotypes covered 97.9% of the total number of haplotypes.

was used to depict the evolutionary history of haplotypes in a phylogram. Power analysis was performed using the Genetic Power Calculator (http://stagen.iop.kcl.ac.uk/gpc/) (45).

ACKNOWLEDGEMENTS

We would like to express our gratitude to all participants in this study. We greatly appreciate the assistance of ophthalmologist H. Fujikura for his expert examinations. We wish to thank Y. Ishituka for his technical assistance and the following psychiatrists for their help in collecting psychiatric patients: T. Kumakura and T. Ichimiya. We would like to thank nurse C. Tachibana for her assistance with physical examinations. This work was supported by RIKEN BSI Funds and Research on Brain Science Funds from the Ministry of Health Labor and Welfare, Japan.

REFERENCES

1. Murray, R.M. and Lewis, S.W. (1987) Is schizophrenia a neurodevelopmental disorder? *Br. Med. J. (Clin. Res. Ed.)*, **295**, 681–682.
2. McNeil, T.F., Cantor-Graae, E. and Ismail, B. (2000) Obstetric complications and congenital malformation in schizophrenia. *Brain Res. Rev.*, **31**, 166–178.
3. Smith, D.W. (1970) *Recognizable Patterns of Human Malformation*. WB Saunders, Philadelphia, PA.
4. O'Callaghan, E., Buckley, P., Madigan, C., Redmond, O., Stack, J.P., Kinsella, A., Larkin, C., Ennis, J.T. and Waddington, J.L. (1995) The relationship of minor physical anomalies and other putative indices of developmental disturbance in schizophrenia to abnormalities of cerebral structure on magnetic resonance imaging. *Biol. Psychiat.*, **38**, 516–524.
5. O'Callaghan, E., Larkin, C., Kinsella, A. and Waddington, J.L. (1991) Familial, obstetric, and other clinical correlates of minor physical anomalies in schizophrenia. *Am. J. Psychiat.*, **148**, 479–483.
6. Ismail, B., Cantor-Graae, E. and McNeil, T.F. (1998) Minor physical anomalies in schizophrenic patients and their siblings. *Am. J. Psychiat.*, **155**, 1695–1702.
7. Waldrop, M.F., Pedersen, F.A. and Bell, R.Q. (1968) Minor physical anomalies and behavior in preschool children. *Child Dev.*, **39**, 391–400.
8. Green, M.F., Satz, P., Gaier, D.J., Ganzell, S. and Kharabi, F. (1989) Minor physical anomalies in schizophrenia. *Schizophrenia Bull.*, **15**, 91–99.
9. Lane, A., Kinsella, A., Murphy, P., Byrne, M., Keenan, J., Colgan, K., Cassidy, B., Sheppard, N., Horgan, R., Waddington, J.L. *et al.* (1997) The anthropometric assessment of dysmorphic features in schizophrenia as an index of its developmental origins. *Psychol. Med.*, **27**, 1155–1164.
10. Engle, E.C. (1998) The genetics of strabismus: Duane, Moebius, and fibrosis syndromes. In Traboulsi, E. (ed.), *Genetic Diseases of the Eye: a Textbook and Atlas*. Oxford University Press, New York, pp. 477–512.
11. Kaufman, M.H. (1992) *The Atlas of Mouse Development*. Academic Press, London, UK.
12. Nakano, M., Yamada, K., Fain, J., Sener, E.C., Selleck, C.J., Awad, A.H., Zwaan, J., Mullaney, P.B., Bosley, T.M. and Engle, E.C. (2001) Homozygous mutations in ARIX(PHOX2A) result in congenital fibrosis of the extraocular muscles type 2. *Nat. Genet.*, **29**, 315–320.
13. Pattyn, A., Morin, X., Cremer, H., Goridis, C. and Brunet, J.F. (1997) Expression and interactions of the two closely related homeobox genes Phox2a and Phox2b during neurogenesis. *Development*, **124**, 4065–4075.
14. Paul, T.O. and Hardage, L.K. (1994) The heritability of strabismus. *Ophthalmic Genet.*, **15**, 1–18.
15. Yokoyama, M., Watanabe, H. and Nakamura, M. (1999) Genomic structure and functional characterization of NBPhox (PMX2B), a homeodomain protein specific to catecholaminergic cells that is involved in second messenger-mediated transcriptional activation. *Genomics*, **59**, 40–50.
16. Amiel, J., Laudier, B., Attie-Bitach, T., Trang, H., de Pontual, L., Gener, B., Trochet, D., Etchevers, H., Ray, P., Simonneau, M. *et al.* (2003) Polyalanine expansion and frameshift mutations of the paired-like homeobox gene PHOX2B in congenital central hypoventilation syndrome. *Nat. Genet.*, **33**, 459–461.
17. Valarche, I., Tissier-Seta, J.P., Hirsch, M.R., Martinez, S., Goridis, C. and Brunet, J.F. (1993) The mouse homeodomain protein Phox2 regulates Ncam promoter activity in concert with Cux/CDP and is a putative determinant of neurotransmitter phenotype. *Development*, **119**, 881–896.
18. Leskowitz, E. (1984) Strabismus and schizophrenia. *Am. J. Psychiat.*, **141**, 614.
19. Krakauer, E.L., Goldstein, L.E., and Wood, S.W. (1995) Schizophrenia and strabismus. *J. Nerv. Ment. Dis.*, **183**, 662–663.
20. Silver, J.M., Yudofsky, S.C. and Hurowits, G.I. (1994) Psychopharmacology and electroconvulsive therapy. In Hales, R.E. Yudofsky, S.C. and Talbott, J.A. (eds), *The American Psychiatric Press Textbook of Psychiatry Second Edition*, 2nd edn. American Psychiatric Press, Inc, Washington, DC, pp. 897–1007.
21. Schlossman, A. (1952) Role of heredity in etiology and treatment of strabismus. *Arch. Ophth.*, **47**, 1–20.
22. Waardenburg, P. (1954) Anomalies of presumable peripheral origin of the extraocular muscles. In Waardenburg, P., Franceschetti, A. and Klein, D. (ed.), *Genetics and Ophthalmology*. Thomas, Springfield, IL, Vol. 2, pp. 10–11.
23. Maumenee, I.H., Alston, A., Mets, M.B., Flynn, J.T., Mitchell, T.N. and Beaty, T.H. (1986) Inheritance of congenital esotropia. *Trans. Am. Ophthalmol. Soc.*, **84**, 85–93.
24. Gover, M. and Yankey, J. (1944) Physical impairments of members of lowincome farm families11, 490 persons. *Pub. Health Rep.*, **59**, 1163–1184.
25. Nordlow, W. (1964) Squint: the frequency of onset at different ages and the incidence of some associated defects in a Swedish population. *Acta Ophthalmol. (Copenh.)*, **42**, 1015–1037.
26. Laatikainen, L. and Erkkila, H. (1980) Refractive errors and other ocular findings in school children. *Acta Ophthalmol. (Copenh.)*, **58**, 129–136.
27. Ing, M. and Pang, S. (1978) The racial distribution of strabismus. *The 3rd Meeting of the International Strabismological Assn.* Grune and Stratton, New York, NY, pp. 107–110.
28. Mallet, J. (1996) The TiPS/TINS lecture. Catecholamines: from gene regulation to neuropsychiatric disorders. *Trends Pharmacol. Sci.*, **17**, 129–135.
29. Pattyn, A., Morin, X., Cremer, H., Goridis, C. and Brunet, J.F. (1999) The homeobox gene Phox2b is essential for the development of autonomic neural crest derivatives. *Nature*, **399**, 366–370.

30. Mundlos, S., Otto, F., Mundlos, C., Mulliken, J.B., Aylsworth, A.S., Albright, S., Lindhout, D., Cole, W.G., Henn, W., Knoll, J.H. *et al.* (1997) Mutations involving the transcription factor CBFA1 cause cleidocranial dysplasia. *Cell*, **89**, 773–779.
31. Goodman, F.R., Bacchelli, C., Brady, A.F., Brueton, L.A., Fryns, J.P., Mortlock, D.P., Innis, J.W., Holmes, L.B., Donnenfeld, A.E., Feingold, M. *et al.* (2000) Novel HOXA13 mutations and the phenotypic spectrum of hand-foot-genital syndrome. *Am. J. Hum. Genet.*, **67**, 197–202.
32. Muragaki, Y., Mundlos, S., Upton, J. and Olsen, B.R. (1996) Altered growth and branching patterns in synpolydactyly caused by mutations in HOXD13. *Science*, **272**, 548–551.
33. Brown, S.A., Warburton, D., Brown, L.Y., Yu, C.Y., Roeder, E.R., Stengel-Rutkowski, S., Hennekam, R.C. and Muenke, M. (1998) Holoprosencephaly due to mutations in ZIC2, a homologue of Drosophila odd-paired. *Nat. Genet.*, **20**, 180–183.
34. Mortlock, D.P., Sateesh, P. and Innis, J.W. (2000) Evolution of N-terminal sequences of the vertebrate HOXA13 protein. *Mamm. Genome*, **11**, 151–158.
35. Krouse, J.P. and Kaufman, J.M. (1982) Minor physical anomalies in exceptional children: a review and critique pf research. *Child Psychol.*, **10**, 247–264.
36. Smalley, S.L., Asarnow, R.F. and Spence, M.A. (1988) Autism and genetics. *Arch. Gen. Psychiat.*, **45**, 953–961.
37. Association, A.P. (1994) *Diagnostic and Statistical Manual of Mental Disorders, 4th edn.* American Psychiatric Association Press, Washington, DC.
38. Yamada, K., Iwayama-Shigeno, Y., Yoshida, Y., Toyota, T., Itokawa, M., Hattori, E., Shimizu, H. and Yoshikawa, T. (2004) Family-based association study of schizophrenia with 444 markers and analysis of a new susceptibility locus mapped to 11q13.3. *Am. J. Med. Genet. (Neuropsychiat. Genet.)*, in press.
39. Johnson, K.R., Smith, L., Johnson, D.K., Rhodes, J., Rinchik, E.M., Thayer, M. and Lewis, E.J. (1996) Mapping of the ARIX homeodomain gene to mouse chromosome 7 and human chromosome 11q13. *Genomics*, **33**, 527–531.
40. Costa, G.L., Bauer, J.C., McGowan, B., Angert, M. and Weiner, M.P. (1996) Site-directed mutagenesis using a rapid PCR-based method. *Methods Mol. Biol.*, **57**, 239–248.
41. Kim, H.S., Seo, H., Yang, C., Brunet, J.F. and Kim, K.S. (1998) Noradrenergic-specific transcription of the dopamine beta-hydroxylase gene requires synergy of multiple cis-acting elements including at least two Phox2a-binding sites. *J. Neurosci.*, **18**, 8247–8260.
42. Dudbridge, F., Koeleman, B.P., Todd, J.A. and Clayton, D.G. (2000) Unbiased application of the transmission/disequilibrium test to multilocus haplotypes. *Am. J. Hum. Genet.*, **66**, 2009–2012.
43. Thompson, J.D., Higgins, D.G. and Gibson, T.J. (1994) CLUSTAL W: improving the sensitivity of progressive multiple sequence alignment through sequence weighting, position-specific gap penalties and weight matrix choice. *Nucl. Acids Res.*, **22**, 4673–4680.
44. Page, R.D. (1996) TreeView: an application to display phylogenetic trees on personal computers. *Comput. Appl. Biosci.*, **12**, 357–358.
45. Purcell, S., Cherny, S.S. and Sham, P.C. (2003) Genetic power calculator: design of linkage and association genetic mapping studies of complex traits. *Bioinformatics*, **19**, 149–150.

The Pharmacogenomics Journal (2004) 4, 114–126

www.nature.com/tpj

ORIGINAL ARTICLE

Comprehensive expression analysis of a rat depression model

N Nakatani[1]
H Aburatani[1,2]
K Nishimura[3]
J Semba[1,4]
T Yoshikawa[1]

[1]*Laboratory for Molecular Psychiatry, RIKEN Brain Science Institute, Wako, Saitama, Japan;* [2]*Department of Cancer Systems Biology, Research Center for Advanced Science and Technology, The University of Tokyo, Tokyo, Japan;* [3]*Department of Information Systems, Research Center for Advanced Science and Technology, The University of Tokyo, Tokyo, Japan;* [4]*The University of the Air, Chiba, Japan*

Correspondence:
Dr T Yoshikawa, Laboratory for Molecular Psychiatry, RIKEN Brain Science Institute, 2-1 Hirosawa, Wako, Saitama 351-0198, Japan.
Tel: +81 48 467 5968
Fax: +81 48 467 7462
E-mail: takeo@brain.riken.go.jp

Received: 20 May 2003
Revised: 03 November 2003
Accepted: 10 December 2003

ABSTRACT

Herein we report on a large-scale analysis of gene expression in the 'learned helplessness' (LH) rat model of human depression, using DNA microarrays. We compared gene expression in the frontal cortex (FC) and hippocampus (HPC) of untreated controls, and LH rats treated with saline (LH-S), imipramine or fluoxetine. A total of 34 and 48 transcripts were differentially expressed in the FC and HPC, respectively, between control and LH-S groups. Unexpectedly, only genes for NADH dehydrogenase and zinc transporter were altered in both the FC and HPC, suggesting limited overlap in the molecular processes from specific areas of the brain. Principal component analysis revealed that sets of upregulated metabolic enzyme genes in the FC and downregulated genes for signal transduction in the HPC can distinguish clearly between depressed and control animals, as well as explain the responsiveness to antidepressants. This comprehensive data could help to unravel the complex genetic predispositions involved in human depression. *The Pharmacogenomics Journal* (2004) 4, 114–126. doi:10.1038/sj.tpj.6500234

Keywords: learned helplessness; DNA microarray; frontal cortex; hippocampus; antidepressant

INTRODUCTION

Depression is a complex psychiatric disease with specific symptoms that include depressed mood, loss of interest, diminished appetite, sleep disturbances and psychomotor retardation. Depression is common, with lifetime prevalence estimated to be up to 20%,[1] and the condition exacts high personal and social costs on sufferers. The illness is also a major cause of suicide. Epidemiological studies suggest a genetic component to affective disorder,[1,2] and efforts to identify susceptibility genes by linkage and other genetic analyses are being conducted.[3] However, the precise etiologies remain elusive, as does the development of new therapies against depression, particularly for cases that are refractory to conventional therapy. In the case of complex trait diseases, isolating genetic mechanisms using human disease material is often difficult because of sample heterogeneity and other confounding factors. Analysis of suitable animal models under strictly controlled conditions would therefore be beneficial.

To investigate the molecular basis of depression, we have applied DNA microarray technology to analyze gene expressions in learned helplessness (LH) rats, an animal model of depression. After pretreatment with repeated inescapable shocks, animals with LH display decreased ability to escape adverse situations. This behavioral model was originally described in dogs,[4] and later analogous behavior was induced in rats.[5] LH animals display behavioral phenotypes resembling human depressive symptoms, and LH can be ameliorated

using antidepressant drugs.[6,7] LH therefore fulfills the parameters of construct validity, face validity and predictive validity,[8] confirming the suitability of the model for studying the neurobiology of depressive illness and the actions of antidepressants.[9–11] It is also important to note that the 'depressive state' in LH animals lasts for over 3 weeks,[12] making this model particularly useful for studying the chronic changes in brain physiology that accompany depression. We examined the frontal cortex (FC) and hippocampus (HPC) of LH rats, because positron emission tomography scanning and functional magnetic resonance imaging studies have recently indicated a potential abnormality in the frontal cortex of both familial bipolar and unipolar depressives.[13] In addition, recent evidence has suggested that neurogenesis in the HPC may be disturbed in depressive patients.[14–16]

In this study, we have analyzed brain transcripts altered during LH and followed their responsiveness to a classical tricyclic antidepressant (TCA), imipramine, and a new generation selective serotonin reuptake inhibitor (SSRI), fluoxetine. In addition, we performed principal component analysis (PCA) to extract essential gene sets from complex expression data sets that can best explain the different pathophysiological conditions. This was achieved by considering genes as variables in PCA. When genes are variables, the analysis creates a set of principal gene components indicating the features of genes that best explain the experimental responses. Using these comprehensive pharmaco-behavioral genetic approaches, we have attempted to generate data that would eventually allow for the formulation of hypotheses to help understand the molecular and genetic pathophysiology of depression. This in turn could lead to the development of novel antidepressants with greater efficacy.

RESULTS AND DISCUSSION

Effectiveness of Antidepressants in Learned Helplessness

The LH model is difficult to generate, requiring meticulous refinement of multiple experimental parameters. In our experimental setting, after inescapable shock pretreatment, animals were subjected to 15 avoidance trials at 30 s intervals. In each trial, a current was applied via the floor grid during the first 3 s. If an animal moved to a neighboring compartment within this period (escape response), the shock was terminated. Failures in escape response were counted as a measure of LH. We defined animals as being in a state of LH when escape failures were demonstrated in more than half of the trials in the session. Using this system, we reproducibly induced LH in rats with a success rate of ~40%. LH rats were subsequently treated with repeated injections of saline (LH-S), fluoxetine (LH-F) or imipramine (LH-I), then re-evaluated for escape responses in the test session. Figure 1 shows a schematic of these procedures. During the escapable shock of the test session, all animals in the LH-S group ($n=10$) showed more than eight escape failures, and the mean failure was significantly higher than that of control rats (those that were not given inescapable shock, $n=15$) (Figure 2). Antidepressant administration significantly reduced the number of escape failures for both LH-F ($P<0.05$) and LH-I ($P<0.01$). Imipramine recovered all

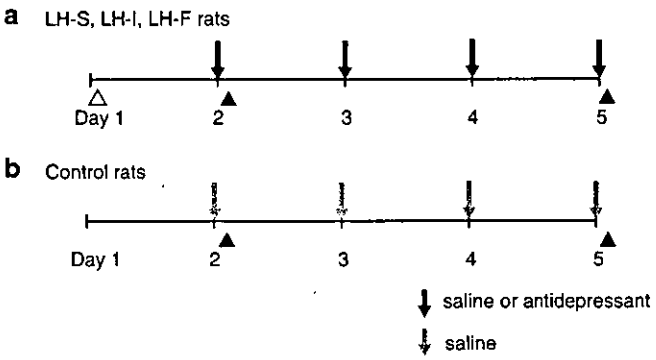

Figure 1 Schematic representation of behavioral procedures. (a) To induce the LH state, animals were given inescapable shock (△) on day 1. On day 2, they received escapable shock (▲), and were selected as 'LH rats' if they showed greater than 50% failure in escape responses. LH animals were then administered saline (LH-S) or antidepressants (LH-F, LH-I) for 4 consecutive days. These animals received escapable shock (▲) again on day 5 to determine whether they were still in the LH state. (b) Control rats were not given inescapable shock on day 1, but treated in the same way thereafter as the LH rats.

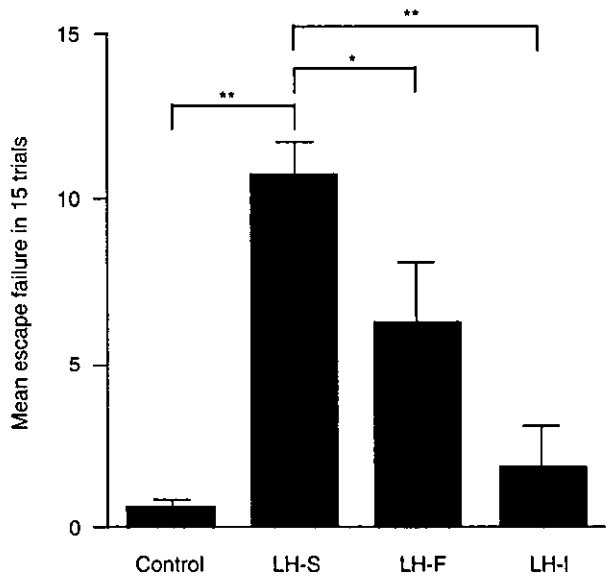

Figure 2 Mean number of escape failures (±SE) during the 15 avoidance trials. Controls ($n=15$) were not given inescapable shocks. Rats exposed to prior inescapable shocks were treated with saline (LH-S) ($n=10$), fluoxetine (LH-F) ($n=7$) or imipramine (LH-I) ($n=9$) once a day for consecutive days (days 2–5). Escape failure refers to the failure of animals to move into the safe compartment during electric footshock (0.5 mA, 3 s duration). The mean numbers of escape failures among groups were evaluated by ANOVA, $F(3,37)=23.69$. $^{*}P<0.01$ and $^{**}P<0.001$ by *post hoc* Tukey–Kramer test.

rats from the LH state ($n=9$), and fluoxetine reinstated five out of seven. These results confirm the persistency of LH in our animals and the effectiveness of antidepressants in this model.[5,17–20] Fluoxetine produced a weaker response compared to imipramine in alleviating the LH phenotype (Figure 2). We also tested larger doses of each drug, 10 mg/kg i.p. of fluoxetine and 50 mg/kg i.p. of imipramine, but did not observe any significant change in the number of escape failures (10 mg/kg of fluoxetine, 5.0 ± 1.0 ($n=3$); 50 mg/kg of imipramine, 2.0 ± 1.3 ($n=3$)) between the two doses. In addition, Anthony *et al*[21] showed that 5 mg/kg of fluoxetine, the same dose as used in the present study, was enough to elicit monoaminergic perturbation such as a reduced 5-hydroxytryptamine receptor 1B expression in the dorsal raphe of rats. Bristow *et al*[22] also demonstrated the validity and efficacy of 5 mg/kg of fluoxetine in ameliorating depressive behavior in rats. We attempted to minimize the nonspecific effects of the drugs by using the lowest possible dose that maintained antidepressive efficacy.

The present results may reflect the different clinical potencies of the individual agents. TCAs such as imipramine inhibit the reuptake of both serotonin and norepinephrine at nerve terminals by acting on monoamine transporters. In contrast, SSRIs including fluoxetine specifically block the reuptake of serotonin.[2] These differences in pharmacological profiles underlie the distinct antidepressive competences exerted by TCA and SSRI. Although human patients require over 2 weeks of medication before antidepressive effects are observed, we administered the drugs for 4 days in our rodent experiments, in keeping with the protocols of Geoffroy *et al*[6] (5-day treatment) and Tordera *et al*[23] (4-day treatment), and could replicate distinct behavioral responses to therapy.

We also measured weight gain during the 5 days of experiments. Weight increase in the LH-S group was significantly lower than that in controls (LH-S, 18.8 ± 4.4 g; control, 31.7 ± 2.2 g; $P<0.05$).

General Profiles of Gene Expressions Associated with LH and Antidepressant Treatments

We selected six animals each from the control (rats showing no escape failure in the escapable shock session) and LH-S groups, and five each from the LH-F and LH-I groups (these showed $\leqslant 7$ failures in the 15 trials), to perform microarray analyses. Patterns of gene expression in the two brain regions from the four rat groups were examined using the Affymetrix GeneChip U34A, which represents 8799 probe sets and codes over 8000 transcripts including known genes (>5000) and expressed sequence tags (ESTs). Transcript expression from extracted RNA displayed good linearity in both FC and HPC samples (Figure 3). Our stringent criteria identified 34 and 48 transcripts as differentially expressed between control ($n=6$) and LH-S ($n=6$) groups in the FC and HPC, respectively (henceforth referred to as 'LH-associated transcripts') (Figures 3a and b). However, none of these transcripts survived after the Benjamin and Hochbery False Discovery Rate analysis. This observation may confirm the statements of Mirnics *et al*[24] that true gene-expression changes in psychiatric traits are small and

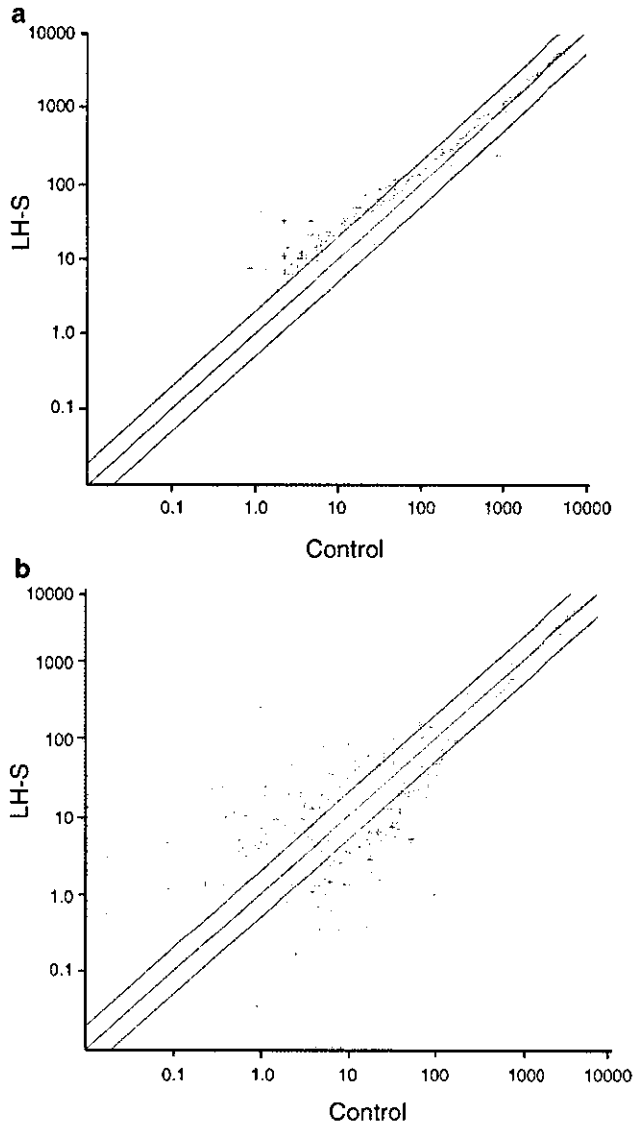

Figure 3 Scatter plot of log-intensity values for the over 8000 genes assayed with the RG-U34A chip in the frontal cortex (a) and hippocampus (b). Each point represents the log value from an average of six control or six LH-S animals.

psychiatric diseases may result from cumulative subtle changes.

Among LH-associated transcripts, five transcripts and one gene showed significant recovery to control levels from the LH state under both imipramine ($n=5$) and fluoxetine ($n=5$) administration in the FC and HPC, respectively (white portions in Figures 4a and b). Transcripts in the pink and yellow areas of Figure 4 represented expression levels that returned to normal after administration of imipramine and fluoxetine, respectively. Interestingly, no LH-associated transcripts demonstrated significant deviation from control levels after drug treatment. That is, none of the LH-associated genes were further decreased or excessively

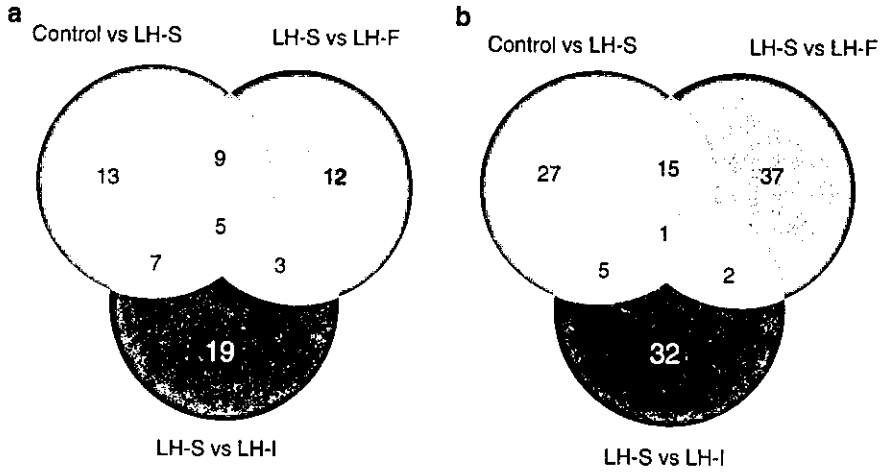

Figure 4 Venn-diagram selection of LH- and antidepressant-associated transcripts in the frontal cortex (a) and hippocampus (b). Comparisons were made between control ($n=6$) and LH-S rats ($n=6$), between LH-S and LH-F rats ($n=5$), and between LH-S and LH-I rats ($n=5$). The LH-I and LH-F rats were those that showed more than 50% success in escape behavior after drug treatments. The number in each compartment denotes the number of differentially expressed transcripts between two groups (see Materials and Methods for a definition of our criteria).

increased after initiating therapy. Approximately 38% of LH-associated transcripts in the FC and 56% in the HPC could not be normalized by either antidepressant (Figure 4; red area). These transcripts could represent the potential targets for novel antidepressants with efficacy against refractory depression. The green, purple and light blue segments in Figure 4 depict the transcripts with expression levels that did not differ between control and LH-S groups, but were significantly altered by fluoxetine, imipramine or both drug treatments, respectively. The information on these transcripts is provided as supplementary Tables S1 and S2. Some of these transcripts may be relevant to the manifestation of adverse reactions by TCA and SSRI. Tables 1 and 2 show the listing of LH-associated transcripts according to putative functions, along with *P*-values between different treatment groups. Data are also provided on the 'average difference' $\pm$SE of each transcript (that corresponds to an absolute value) in supplementary Tables S1 and S2. In all, 17 known genes and one EST showed downregulation (marked in red), whereas 16 transcripts including ESTs were upregulated in the FC (Table 1). In contrast, the majority of known LH-associated genes in the HPC were downregulated (27 of 31) (marked in red in Table 2). Even allowing for ESTs, the number of downregulated transcripts in the HPC significantly exceeds the upregulated transcripts (32 *vs* 16) (Table 2).

We chose four genes from each of Tables 1 and 2, and examined mRNA levels in the same RNA samples used for microarray experiments under 'one-step' quantitative RT-PCR reactions (Table 3). These results showed the same direction of expressional changes seen in the microarray experiments, but less correlation was found with the degree of change between the two methods, as indicated in prior studies.[25,26] Furthermore, since only a limited number of transcripts were confirmed by independent methods and no transcripts were confirmed when Bonferroni's correction was applied to the quantitative RT-PCR results, the present DNA microarray data are broadly unconfirmed.

LH-associated Transcripts in the FC

When classified according to function, genes defined as receptors or ion channel/transporters were all downregulated in LH animals (Table 1). Among them, the serotonin receptor type 2A (*Htr2a*) gene showed a 1.6-fold decrease, and recovery with both fluoxetine and imipramine. Evidence from other animal models for depression[27,28] and clinical observations[29] have also suggested a pathological role for *HTR2A* in the depressive state. The change in inositol-1,4,5-triphosphate receptor type 1 (*Itpr1*) level was small, but statistically significant. Both types of antidepressant normalized the reduced expression of *Itpr1*. The observed decrease in both *Htr2a* and *Itpr1* and their restitution to original levels by antidepressants is in keeping with a proposed theory of dysregulated monoamine-mediated calcium signaling in depression.[30,31] Other members of the receptor and ion channel/transporter gene families that showed restoration with fluoxetine or imipramine included a voltage-gated potassium channel and zinc transporter (Table 1). Conversely, three genes from the signal transduction family were all upregulated in LH-S rats compared to controls (Table 1). Of interest is prostaglandin D synthase, an enzyme that produces prostaglandin D_2, a potent endogenous sleep-promoting substance.[32] This enzyme has recently been implicated in the regulation of nonrapid eye movement (NREM).[33] Sleep disturbance is a typical symptom of human depression. Examination of sleep parameters in LH rats, particularly the NREM period, would therefore be of interest. Protein kinase C epsilon (PKCε), which is a member of nPKC, showed a small but significant increase in LH-S compared with controls.

Table 1 LH-associated transcripts in the frontal cortex

Functional Groups	*Fold change*[a]	*P-value*[b]			*Accession no.*
		Cont vs LH-S	*LH-S vs LH-F*	*LH-S vs LH-I*	
Receptor					
Inositol-1,4,5-triphosphate receptor type I	−1.1	0.0032	0.0078	0.0078	J05510
Serotonin receptor 2A	−1.6	0.0479	0.0352	0.0358	M64867
Ion channel/Transporter					
Voltage-gated potassium channel	−1.1	0.0289	0.0078		X62840
Dri 27/ZnT4 (zinc transporter)	−1.3	0.0289		0.0026	Y16774
Cl-/HCO3- exchanger (B3RP2)	−1.4	0.0484			J05166
Signal transduction					
Prostaglandin D2 synthetase	1.3	0.0484	0.0006	0.0181	J04488
PKC epsilon	1.2	0.0158	0.0181		M18331
Neurexophilin 4	2.0	0.0156			AF042714
Neural growth/ structure					
Tau	−1.1	0.0479	0.0358		X79321
Jagged2 precursor	1.3	0.0158		0.0358	U70050
Similar to cdc37	1.6	0.0484			D26564
MAP2	−1.4	0.0158			S74265
I136-alpha7 integrin alpha chain	−1.5	0.0289			X65036
Neu differentiation factor	−1.6	0.0484			M92430
LIMK-1	−9.5	0.0436			D31873
Metabolic enzymes					
Thioradoxin reductase 1	−1.2	0.0011	0.0181		AA891286
F1-ATPase epsilon subunit	1.1	0.0011		0.0026	AI171844
Mitochondrial fumarase	−1.1	0.0110		0.0181	J04473
Lipoprotein lipase	1.5	0.0484			L03294
24-kDa subunit of mitochondrial NADH dehydrogenase	1.4	0.0484			M22756
Bleomycin hydrolase	1.4	0.0158			D87336
Stress response					
Rapamycin and FKBP12 target-1 protein (rRAFT1)	1.1	0.0158	0.0358		U11681
Neuronal death protein	2.3	0.0484			D83697
Poly(ADP-ribose) polymerase	1.6	0.0077			U94340
Others					
Taipoxin-associated calcium binding protein-49 precursor	−1.2	0.0032	0.0119		U15734
Cytosolic resiniferatoxin binding protein RBP-26	−1.3	0.0289	0.0358		X67877
RNA binding protein (transformer-2-like)	−1.2	0.0110	0.0181		D49708
C15	−1.2	0.0002		0.0006	X82445
resection-induced TPI (rs11)	1.4	0.0011			AF007890
Anti-proliferative factor (BTG1)	−1.4	0.0484			L26268
Unknown					
EST	−1.5	0.0158	0.0474	0.0026	AA892280
EST	1.2	0.0484	0.0026		AI230632
EST	1.4	0.0484		0.0078	AA894234
EST	1.2	0.0484		0.0181	AF069782

[a]The fold change was calculated between mean values of control ($n = 6$) and LH-S rats ($n = 6$). Positive values indicate an increase, and negative a decrease in gene expression in the LH.
[b]Statistical comparison was made by Mann-Whitney test (two-tailed). Only significant *P*-values (< 0.05) are denoted.

Activation of serotonin 2 receptors reportedly diminished γ-amino butyric acid type A receptor current through PKC in prefrontal cortical neurons.[34] Expression changes in the *Htr2a* and PKCε genes in LH may indicate a functional link between the two systems in the depressive state. The precise role of neurexophilin 4 in the intercellular signaling system remains unclear,[35,36] but the gene may underlie a depression/stress-related physiological pathway that cannot be corrected using TCAs or SSRIs (Table 1).

Of the LH-associated genes identified from the FC, LIMK-1 (LIM domain kinase 1: *Limk1*) displayed the most dramatic decrease, a 9.5-fold reduction compared with control levels (Table 1). Transcriptional levels were not completely normalized by imipramine or fluoxetine treatment. This

Table 2 LH-associated transcripts in the hippocampus

Functional Groups	*Fold change*[a]	*P-value*[b]			*Accession No.*
		Cont vs LH-S	*LH-S vs LH-F*	*LH-S vs LH-I*	
Receptor					
HGL-SL1 olfactory receptor pseudogene	−2.0	0.0005	0.0358		AF091574
olfactory receptor-like protein (SCR D-9)	−1.4	0.0050			AF034899
heparin-binding fibroblast growth factor receptor 2	−2.4	0.0373			L19112
HFV-FD1 olfactory receptor	−2.5	0.0019			AF091575
Ion channel/Transporter					
Dri 27/ZnT4 protein (zinc transporter)	1.2	0.0464	0.0181		Y16774
Chloride channel RCL1	−1.1	0.0373	0.0181		D13985
High-Affinity L-proline transporter	−1.3	0.0050		0.0078	M88111
Plasma membrane CA2+-ATPase isoform 3	−1.4	0.0018			M96626
Signal transduction					
Paranodin	1.2	0.0213	0.0078		AF000114
Arl5 (ADP-ribosylation factor-like 5)	1.4	0.0213			AA956958
Grb14	−1.4	0.0213			AF076619
Neurotransmission					
Synuclein SYN1	−1.2	0.0213	0.0358		S73007
Alpha-soluble NSF attachment protein	1.1	0.0213		0.0078	X89968
Rab13	−1.9	0.0005		0.0358	M83678
Rab3b	−1.6	0.0213			AA799389
GTP-binding protein (ral B)	2.0	0.0110			L19699
Neural growth/ structure					
Tuba1 (Alpha-tubulin)	1.2	0.0213	0.0006		AA892548
Zinc-finger protein AT-BP2	−1.4	0.0213			X54250
CRP2 (cysteine-rich protein 2)	1.4	0.0373			D17512
Nfyb CCAAT binding transcription factor of CBF-B/NFY-B	1.4	0.0373			AA817843
Decorin	2.2	0.0213			AI639233
Metabolic enzymes					
NADH-cytochrome b-5 reductase	1.1	0.0110	0.0358	0.0181	AI229440
Siat5 (Sialyltransferase 5)	1.7	0.0050	0.0078		X76988
24-kDa mitochondrial NADH dehydrogenase precursor	−1.4	0.0373			M22756
2-oxoglutarate carrier	−1.4	0.0110			U84727
Soluble cytochrome b5	−1.5	0.0110			AF007107
Stress response					
Ischemia responsive 94 kDa protein (irp94)	−1.4	0.0050			AF077354
MHC class I antigen	1.5	0.0373			AF074609
Others					
RNA splicing-related protein	−1.4	0.0373			AI044739
Aes Amino-terminal enhancer of split	−1.4	0.0153			AA875427
Proteasome RN3 subunit	−1.5	0.0110			L17127
Unknown					
EST	1.5	0.0274	0.0358		AA799488
EST	1.4	0.0373	0.0078		AA858617
EST	1.2	0.0213	0.0026		AA892817
EST	1.2	0.0050	0.0026		AA892238
EST	1.1	0.0213	0.0026		AA799893
EST	1.1	0.0050	0.0006		AA799784
EST	1.5	0.0213	0.0358		AA799525
EST	1.3	0.0373		0.0078	AA893039
EST	1.1	0.0373		0.0358	AI007820
EST	1.3	0.0373		0.0358	AA875348
EST	2.4	0.0213			AA875633
EST	1.9	0.0373			AI229655
EST	1.5	0.0373			AA955477
EST	1.5	0.0213			AA893569
EST	1.4	0.0464			AA800803
EST	−1.6	0.0274			AI639477
EST	1.6	0.0110			AA892353

[a]The fold change was calculated between mean values of control ($n=6$) and LH-S rats ($n=6$). Positive values indicate an increase, and negative values (in red) a decrease in gene expression in the LH.
[b]Statistical comparsion was made by Mann-Whitney test (two-tailed). Only significant *P*-values (<0.05) are denoted.

Table 3 Gene expression levels evaluated by quantitative RT-PCR and comparisons with the results from microarray analysis

	Frontal cortex				*Hippocampus*			
	LIMK-1	*HTR2A*	*PGDS*	*IP3R*	*SNAP*	*SYN1*	*bFGFR2*	*Ca^{2+}-ATPase*
Control	1.00±0.42	1.00±0.57	1.00±0.19	1.00±0.48	1.00±0.36	1.00±0.44	1.00±0.21	1.00±0.31
LH-S	0.49±0.07	0.36±0.06	1.64±0.25[a]	0.97±0.20	0.61±0.14	0.54±0.17	0.88±0.23	0.80±0.37
LH-F	0.50±0.06	0.57±0.26	1.10±0.20	0.52±0.15	0.86±0.14	0.65±0.23	0.65±0.11	0.80±0.14
LH-I	0.44±0.08	0.53±0.08[b]	0.81±0.33	0.72±0.23	1.45±0.51	0.30±0.07	0.52±0.16	0.70±0.29
Fold change evaluated by RT-PCT (Cont *vs* LH-S)	−2.0	−2.8	1.6	−1.0	−1.6	−1.9	−1.1	−1.3
Fold change evaluated by microarray (Cont *vs* LH-S)	−9.5	−1.6	1.3	−1.1	−1.1	−1.2	−2.4	−1.4

The expression level of each gene is normalized to that of the GAPDH gene (mean±SE, $n=6$, each in control and LH-S, $n=5$, each in LH-F and LH-I). The gene abbreviations are: LIMK-1, LIM domain kinase 1; HTR2A, 5-hydroxytryptamine (serotonin) receptor 2A; PGDS, prostaglandin D synthetase; IP3R, inositol-1,4,5-triphosphate receptor type 1; SNAP, synaptosomal-associated protein; SYN1, synuclein 1; bFGFR2, heparin-binding fibroblast growth factor receptor 2; Ca^{2+}-ATPase, plasma membrane Ca^{2+}-ATPase isoform 3.
[a]$P<0.05$ (control *vs* LH-S).
[b]$P<0.05$ (LH-S *vs* LH-I) by Mann–Whitney test (two-tailed).

partial recovery might be due to the low level of normal transcription and the large variation of expression values (supplementary Table S3). We therefore performed real-time RT-PCR to confirm the expression profile of *Limk1*, and detected a two-fold decrease in LH compared to control animals. This reduction was not recovered by antidepressant treatments (Table 3). *Limk1* is expressed in both fetal and adult nervous systems, and shows ubiquitous expression in the brain with the strongest expression in adult cerebral cortex.[37] Recently, *Limk1*-knockout mice were reported to show abnormalities in spine morphology and enhanced long-term potentiation, accompanied by alterations in fear response and spatial learning.[38] A test of depression-related behavioral parameters in these mice would be intriguing. Additional reports that depressive patients frequently manifest subcortical hyperintensity near frontal white matter ('myelin pallor' on histological examination)[39] suggest that LIMK1 may be involved in an as yet undetermined intercellular signaling pathway disrupted in depression, as LIMK1 is known to phosphorylate myelin basic proteins.[40]

Our criteria for selecting 'altered' transcripts in LH compared to control animals may have been conservative and inadvertently excluded many potential candidates. Decreased levels of brain-derived neurotrophic factor (BDNF) recoverable by antidepressant treatment have been reported in patients with depression.[41,42] Although we could not detect any significant difference in expression between control and LH-S animals, we found that expression of BDNF in the FC was increased in LH-I animals compared with LH-S and control animals (supplementary Table S3).

LH-associated Transcripts Specific to the HPC and Common to Both the FC and HPC

In contrast to the FC, most LH-associated genes in the HPC showed decreased expressions on the induction of LH (Table 2). Genes coding for receptors were downregulated in both regions, although there was no overlap between the two groups of receptors. This category included three olfactory receptor-like genes, *HGL-SL1* olfactory pseudogene, olfactory receptor-like protein (*SCRD-9*) and *HFV-FD1* olfactory receptor. Although these are thought to encode G protein-coupled receptors with seven transmembrane domains, the biological functions are unclear. Heparin-binding fibroblast growth factor receptor 2 (*Fgfr2*) genes were also downregulated in LH-S, but were unaffected by antidepressants (Table 2). We also found a reduction in the *N*-methyl-D-aspartate receptor 2A (NMDAR 2A) subunit gene in three of six LH-S animals. Fgfr2 reduces NMDAR 2A subunit mRNA levels via a receptor-mediated mechanism.[43] Chronic administration of antidepressants decreases the expression of NMDA receptor subunit genes and radioligand binding to the receptor.[42] This discrepancy warrants further investigation, to determine the role of this growth factor and the NMDA receptor genes in depression. All the LH-associated genes defined as involved in neurotransmission were also downregulated in this study (Table 2). The hippocampus is well known as a region of the brain that is highly susceptible to stress.[44,45] Recent studies have demonstrated that repeated stress causes shortening and debranching of dendrites in the CA3 region of the HPC and suppresses neurogenesis of granule neurons in the dentate gyrus.[45,46] In addition, chronic antidepressant treatment increases cell populations and neurogenesis in the rat hippocampus.[15] The extensive suppression of gene expression observed in our LH model may be related to phenotypic changes in the hippocampus produced by stress.

An unexpected finding was the scarcity of common transcripts between the two areas of brain. Of the LH-associated genes, only those coding for the 24-kDa mitochondrial NADH dehydrogenase and Dri27/ZnT4 (zinc transporter) were common to both the FC and HPC (Tables 1 and 2). However, the direction of change differed between the two regions. This selectivity was also seen in genes that were not affected by LH, but displayed a response to

Table 4 List of genes contributing to the first component in principal component analysis

Brain region[a]	*Eigenvalue*	*Gene name*[b]	Function[c]	*Fold change*	*Accession no*	Locus[d]
Frontal cortex	0.2197	Rapamycin and FKBP12 target-1 protein (rRAFT)	Stress response	1.1	U11681	5q36
	0.2194	F1-ATPase epsilon subunit	Metabolic enzyme	1.1	AI171844	20q13.3
	0.1965	Jagged2 precursor		1.3	U70050	14q32
	0.1929	24-kDa subunit of mitochondrial NADH dehydrog	Metabolic enzyme	1.4	M22756	18p11.31-p11.2
	0.1876	Bleomycin hydrolase	Metabolic enzyme	1.4	D87336	17q11.2
	0.1820	EST	Unknown	1.4	AA894234	—
	0.1760	Poly(ADP-ribose) polymerase	Stress response	1.6	U94340	1q41-q42
	0.1617	EST	Unknown	1.2	AI230632	—
	0.1531	Resection-induced TPI (rs11)	Others	1.4	AF007890	12p13
	0.1525	EST	Unknown	1.2	AF069782	—
Hippocampus	0.2114	HGL-SL1 olfactory receptor pseudogene		−2.0	AF091574	—
	0.2092	Proteasome RN3 subunit	Others	−1.5	L17127	1q21
	0.2019	24-kDa mitochondrial NADH dehydrogenase prec	Metabolic enzyme	−1.4	M22756	18p11.31-p11.2*
	0.1997	HFV-FD1 olfactory receptor		−2.5	AF091575	—
	0.1983	Soluble cytochrome b5	Metabolic enzyme	−1.5	AF007107	18q23*
	0.1865	2-Oxoglutarate carrier	Metabolic enzyme	−1.4	U84727	17p13.3
	0.1845	Grb14	Signal transduction	−1.4	AF076619	2q22-q24
	0.1626	EST	Unknown	−1.6	AA892353	—
	0.1606	GTP-binding protein (ral B)	Signal transduction	−2.0	L19699	2cen-q13
	0.1595	Rab3b	Signal transduction	−1.6	AA799389	1p32-p31*

[a]The 10 largest contributing genes to the first component in each region are listed.

[b]The genes in black indicate those up-regulated in LH animals compared to controls, while genes in red are down-regulated.

[c]The gene functions are color coded according to functional properties.

[d]*indicates that the chromosomal region shows genetic linkage to bipolar disorder.

treatment with fluoxetine, imipramine or both. In this case, from the three subsets (green, light blue and purple areas in Figure 4), five of 105 transcripts were common to both the FC and HPC (supplementary Tables S3 and S4). These findings may highlight region-specific molecular mechanisms involved in the etiology of LH. In human studies, decreased mitochondrial function was demonstrated in the basal ganglia of chronic schizophrenics,[47,48] and inhibition of mitochondrial respiratory complex I activity was reported as a cellular pathology of Parkinson's disease.[49,50] Evidence, including that of decreased ATP in frontal lobes detected in depressive patients,[51] has generated speculation about the role of mitochondrial dysfunction in depression.[52,53] NADH dehydrogenase is located on human chromosome 18 at p11.31–p11.2, a susceptibility region for affective disorder and schizophrenia.[3,54,55] These data suggest a possible link between mitochondrial NADH dehydrogenase and neuropsychiatric illnesses, including depression. The observed alteration in levels of a zinc transporter gene may tie in with recent reports that zinc exerts an antidepressant-like effect in the rodent forced swimming test,[56] and that patients with major depression demonstrate lower serum zinc levels.[57] This may imply perturbed zinc metabolism in depression, but the precise mechanisms are poorly understood.

Given that imipramine was more effective in improving LH behavior than fluoxetine, it may seem contradictory that a larger number of LH-associated transcripts showed a greater response to fluoxetine than to imipramine (Figure 4). Imipramine-responsive transcripts are likely to play a more pivotal role in behavioral recovery.

We also applied parametric statistical analysis (Student's *t*-test) to our array data. The total number of transcripts detected was slightly lower in both the FC and HPC compared to numbers detected by nonparametric tests (3 and 12 fewer in the FC and HPC, respectively). Between the two statistical methods, 10 genes in the FC (32%) and three genes in the HPC (8%) were different (supplementary Tables S7 and S8).

PCA on Altered Transcripts

PCA is a mathematical technique that exploits essential factors to define patterns in data, reducing the effective dimensionality of gene-expression space without significant loss of information.[58] This technique can be applied to both genes and experiments as a means of classification. When genes are variables, the analysis creates a set of principal gene components highlighting features of genes that best explain their experimental responses. We used the LH-associated transcripts from the FC and HPC separately as variables in PCA, to allow for better visualization of the region-specific data sets. Figures 5a and b indicate the eigenvalue distributions on the components in the FC and HPC samples, respectively. The sudden drop in eigenvalues with increasing component number suggests that it is possible to select a small number of components modeling the gene-expression differences among rat groups. We chose a three-component model for both the FC and HPC, which

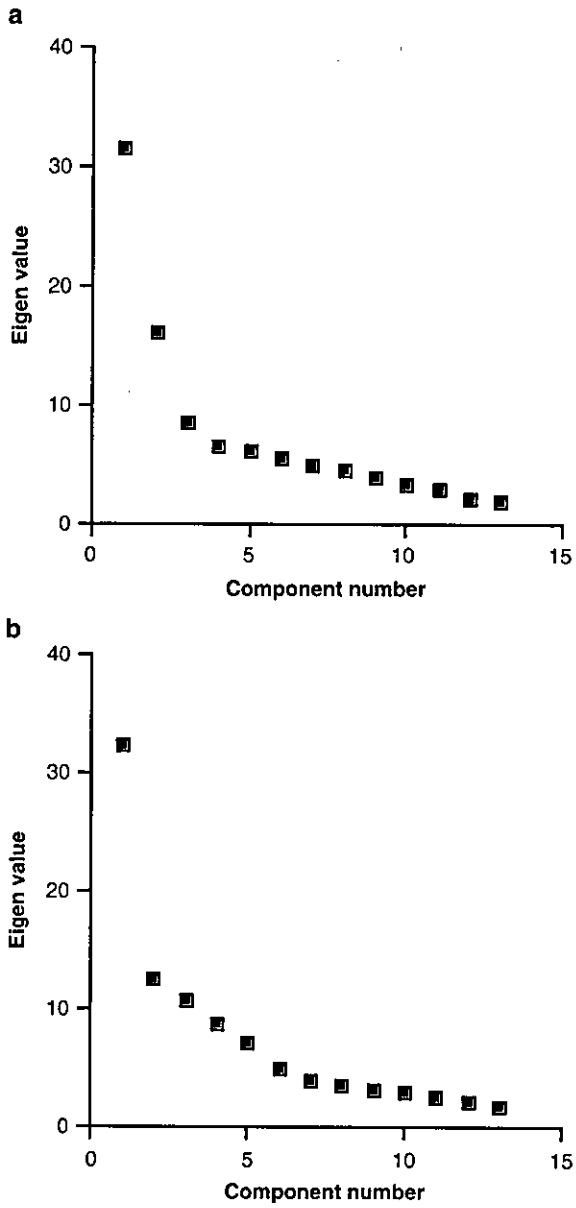

Figure 5 Component number *vs* eigenvalue in the FC (a) and the HPC (b).

explained 56% of the total variability seen in the 34 transcripts from the FC and the 48 transcripts from the HPC. The extracted dimensions represent the linear organization of data from independent systems. Each animal was plotted in a three-dimensional subspace (Figures 6a and b). The first components retain the maximal amount of correlated information (ie coordinated activity of genes) restricting the uncorrelated information to higher order components. In the FC, the first component (axis) showed good separation for the four experimental groups (control, LH-S, LH-F and LH-I), placing the antidepressant-treated groups between the control and LH-S groups. Table 4 shows

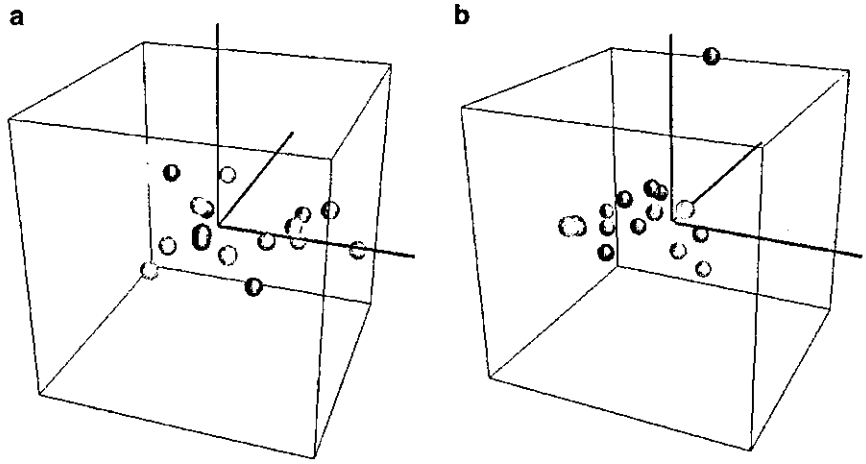

Figure 6 All animals were plotted with respect to the first (blue), second (green) and third (red) principal components. PCA was performed on transcripts listed in Table 1 (frontal cortex) (a) and Table 2 (hippocampus) (b). Yellow-colored dots represent control animals, green LH-S rats, red LH-F and blue LH-I.

transcripts from the FC that were arranged according to the magnitude of correlation with the first component (PC1) (those to the second and third components are shown in supplementary Table S5). They comprised genes for metabolic enzymes and stress responses. All genes listed in PC1 were increased in LH animals compared to controls. Among the genes coding for metabolic enzymes, the F1-ATPase epsilon subunit and 24-kDa subunit of mitochondrial NADH dehydrogenase are both localized to the mitochondria, further suggesting an important role for mitochondrial function in depression.[53] The second and third components in the FC did not further subdivide the experimental groups (supplementary figure S1). However, based on the data including the second component of PCA in the FC (supplementary Table S5), we speculate that genes responsible for neuronal growth and structure including *Limk1* could be key factors in depression/stress-related pathology. In downstream pathways, alterations of these genes may affect recruitment and maintenance of multiple neurotransmitter receptors.[38] In support of this theory, structural abnormalities have recently been reported in the frontal lobe white matter of depressive patients.[59]

According to PC1 in the HPC, LH-S rats were separated from controls, with the drug-treated animals being more closely localized than the LH-S group (Figure 6b). This highlights the limited efficacy of TCA and SSRI antidepressants against dysregulated genes in the HPC, although these drugs reversed the behavioral phenotype of LH rats. The genes contributing to PC1 from the HPC would therefore represent suitable targets for future novel antidepressants. PC1 in the HPC contained genes that were downregulated in LH rats and were clustered as metabolic enzyme and signal transduction (Table 4). The second component in the HPC detected eight genes that correlated with responsiveness to fluoxetine (supplementary Table S6 and Figure S2). One animal was separated from the others along the third component (Figure 6b). The reason for this was not clear. The animal may have suffered from highly aberrant expression of metabolic enzyme- and signal transduction-related genes and other transcripts (Table 4). Finally, the fact that the 24-kDa subunit of mitochondrial NADH dehydrogenase was extracted from both the FC and HPC with high eigenvalues is intriguing, suggesting that this gene may represent an indicator of depressive state. Moreover, the two genes, for soluble cytochrome b5 on 18q23 and Rab3 on 1p32-p31, mapped to reported linkage regions for bipolar disorder.[60]

MATERIALS AND METHODS

Animals and Experimental Design

Male Sprague–Dawley rats, 5–6-week old, weighing 150–180 g, were purchased from SLC (Shizuoka, Japan). They were housed three per cage under standard laboratory conditions, with access to food and water *ad libitum*. After 1 week of handling, the animals were used for experiments. Antidepressants, imipramine and fluoxetine were purchased from SIGMA (St Louis, MO, USA).

On day 1, animals were subjected to IS pretreatment (0.5 mA, 10 s duration, shock interval 1–5 s, 160 trials) in a Plexiglas chamber ($460\,W \times 200\,D \times 180\,H\,mm^3$, Muromachi, Tokyo, Japan). Two rats were processed simultaneously using two chambers. Control rats were placed for 1 h in the same chambers, but no shocks were administered.

On day 2, to evaluate escape and avoidance performance, avoidance training was initiated 24 h after IS pretreatment in the same chamber, which had been converted to a two-way shuttle box by dividing it into two equal-sized compartments using an aluminum partition. The partition included a square gate ($6 \times 6\,cm^2$), through which animals

could move into the adjacent compartment. Animals were subjected to 15 avoidance trials with 30 s intervals. In each trial, 0.5 mA of current was applied via the grid floor during the first 3 s. If an animal crossed the gate and moved to the other compartment within this period (escape response), the shock was terminated. Failures in escape response were counted as a measure of LH. Animals were defined as suffering from LH when they showed eight or more failures during a session. Control rats and a proportion of LH rats (LH-S) were administered saline once a day for three consecutive days, starting on day 2 after the avoidance trial. The remaining LH animals were treated using either imipramine (25 mg/kg, i.p.) (LH-I) or fluoxetine (5 mg/kg, i.p.) (LH-F).

On day 5, 30 min after the final injection, rats were tested for escape ability under escapable shock conditions. Among LH-I and LH-F rats, only those animals that showed a $>50\%$ successful escape response (ie <8 failures in the 15 trials; all LH-I rats fulfilled this criterion) were used for gene-expression analysis.

The present protocol was approved by the RIKEN animal committee.

RNA Preparation and Array Hybridization

Animals were killed on day 6, 24 h after the final electroshock procedure. Total RNA was extracted from the FC (defined as the region anterior to the genu of corpus callosum, with the ventral olfactory structures depleted) and HPC using an acid guanidium thiocyanate/phenol chloroform extraction method (ISOGEN, NIPPON Gene, Toyama, Japan). Double-stranded cDNA was synthesized from 10 μg of total RNA using the SuperScript Choice System (Invitrogen, Carlsbad, CA, USA) and a primer containing poly (dT) and a T7 RNA polymerase promoter sequences (Geneset, La Jolla, CA, USA). Biotin-labeled cRNA was synthesized from cDNA using an Enzo BioArray High Yield RNA Transcript Labeling kit (Enzo Diagnostics, Santa Clara, CA, USA). After fragmentation, 15 μg of cRNA was hybridized for 16 h at 45°C to a U34A chip (Affymetrix, Santa Clara, CA, USA) that contained probes for over 8000 transcripts, including all known rat genes (http://www.affymetrix.com/products/netaffx.html). After hybridization, arrays were washed automatically and stained with streptavidin–phycoerythrin using the fluidics system. Chips were scanned using a GeneArray scanner (Affymetrix).

Data Analysis

All samples were scaled to a target intensity of 100. Data analysis was performed using Microarray Suite 4.0 (Affymetrix) and GeneSpring 4.1 (Silicon Genetics, Redwood, CA, USA). Transcripts with an 'average difference' (as described in the GeneChip software) of <20 for each probe set in controls were excluded (5157 genes were selected out of 8799). From the remaining transcripts, those that gave an 'absolute call' of 'P' (present) for at least four samples in six for control and LH-S rats were considered for further analysis (3541 genes were chosen).

Before statistical analysis, each transcript was converted into a logarithmic value and normalized to itself by making a synthetic positive control and dividing all measurements by this control, assuming that the control value was at least 0.01. A synthetic control is the median of the transcript's expression values over all the samples. Two-group comparison was conducted for each transcript by a Mann–Whitney test between: (i) control and LH-S groups, (ii) LH-S and LH-F groups and (iii) LH-S and LH-I groups. The results are illustrated as a Venn diagram (Figure 2), where the overlapping areas representing (i)-, (ii)- and (iii)-type comparisons include transcripts that were selected solely using Mann–Whitney test ($P<0.05$) and Student's *t*-test ($P<0.05$). Transcripts in non-overlapping areas represent genes whose expressional changes between the two states displayed $\geqslant 1.4$-fold difference, in addition to fulfilling the *P*-value criteria. We also evaluated these selected transcripts by implementing the Benjamin and Hochbery False Discovery Rate program included in the GeneSpring software package. The differential gene expressions revealed by the microarray chips were examined using real-time quantitative reverse transcription (RT)-PCR, with a LightCycler and RNA Amplification kit SYBR Green I (Roche, Basel, Swizerland).

Principal Component Analysis

PCA is a statistical method for determining the coordinate transformation that explains the maximum amount of variance for the data.[25] PCA finds the principal components and each component is mutually orthogonal. To calculate the transformation, data were first normalized with reference to each gene, and then sample mean and sample variance–covariance matrix S were calculated from estimates of the mean and variance–covariance matrix. From this symmetrical matrix S, an orthogonal basis was calculated by determining eigenvalues and eigenvectors according to the equation:

$$|S - \lambda_i E| = 0 \quad (1)$$

where E is an identity matrix and λ_i is the ith eigenvalue. i takes the value (1 to n), and n is the total number of genes.

$$SA_i = \lambda_i A_i \quad (2)$$

where A_i is the ith eigenvector (n-dimension). The first and ith principal components were calculated as follows: $PC1 = \sum A_1 D$, $PCi = \sum A_i D$, where A_1 is the eigenvector with maximum eigenvalue, and D is the n-dimensional data vector. The proportion of the ith component was the ith eigenvalue divided by the total sum of all eigenvalues. Animals were projected into the first three-dimensional component space.[62,63]

CONCLUSION

In an effort to better understand the molecular and genetic bases underlying the pathophysiology of depressive disorder and to improve the rationale for the design of antidepressant drugs, we have performed DNA microarray analysis using an animal model of depression. Using Affymetrix GeneChip arrays, we have screened over 8000 rat genes and

ESTs, and identified 82 distinct transcripts (Tables 1 and 2, and supplementary Tables S1 and S2) in the FC and HPC that are relevant to LH and responsive to conventional antidepressants. To date, the strategy for designing antidepressive drugs is based on the serendipitous paradigm that the augmentation of monoaminergic activity in the central nervous system leads to therapeutic benefits.[1] However, currently available drugs have several drawbacks in terms of slow onset of action and intractable disease presents in approximately one-third of all depressive patients.[61] Given the genetically complex nature of human depression, we recognize that the present study can explain only limited aspects of depression pathology. Nevertheless, we believe that this study could give rise to new ideas for probing into the genetic mechanisms of human affective disorder and for refining the development of advanced therapeutics.

DUALITY OF INTEREST

None declared

ACKNOWLEDGEMENTS

We would like to thank Shuichi Tsutsumi and Hiroko Meguro for assistance with microarray data analysis, Yuichi Ishitsuka, Yuki Iijima and Shin-ichi Ohno for help with animal experiments, Kazuo Yamada for useful comments and Joanne Meerabux for critical reading of this manuscript. This study was partly supported by Grants-in-Aid for Young Scientists (B) (No. 13770566) from the Ministry of Education, Culture, Sports and Technology (MEXT).

ABBREVIATIONS

BDNF	*brain-derived neurotrophic factor*
EST	*expressed sequence tag*
FC	*frontal cortex*
HPC	*hippocampus*
IS	*inescapable shocks*
LH	*learned helplessness*
LH-F	*LH rats treated with fluoxetine*
LH-I	*LH rats treated with imipramine*
LH-S	*LH rats treated with saline*
NMDA	*N-methyl-D-aspartate*
NREM	*nonrapid eye movement*
PKC	*protein kinase C*
RT	*reverse transcription*
SSRI	*selective serotonin reuptake inhibitor*
TCA	*tricyclic antidepressant*

SUPPLEMENTARY INFORMATION

Supplementary Information accompanies the paper on the TPJ website (http://www.nature.com/tpj).

REFERENCES

1 Nestler EJ, Barrot M, DiLeone RJ, Eisch AJ, Gold SJ, Monteggia LM. Neurobiology of depression. *Neuron* 2002; **34**: 13–25.
2 Fava M, Kendler KS. Major depressive disorder. *Neuron* 2000; **28**: 335–341.
3 Detera-Wadleigh SD, Badner JA, Berrettini WH, Yoshikawa T, Goldin LR, Turner G *et al.* A high-density genome scan detects evidence for a bipolar-disorder susceptibility locus on 13q32 and other potential loci on 1q32 and 18p11.2. *Proc Natl Acad Sci USA* 1999; **96**: 5604–5609.
4 Overmier JB, Seligman ME. Effects of inescapable shock upon subsequent escape and avoidance responding. *J Comp Physiol Psychol* 1967; **63**: 28–33.
5 Telner JI, Singhal RL. Psychiatric progress. The learned helplessness model of depression. *J Psychiatr Res* 1984; **18**: 207–215.
6 Geoffroy M, Scheel-Kruger J, Christensen AV. Effect of imipramine in the 'learned helplessness' model of depression in rats is not mimicked by combinations of specific reuptake inhibitors and scopolamine. *Psychopharmacology* 1990; **101**: 371–375.
7 Nankai M, Yamada S, Muneoka K, Toru M. Increased 5-HT2 receptor-mediated behavior 11 days after shock in learned helplessness rats. *Eur J Pharmacol* 1995; **281**: 123–130.
8 Willner P. A Psychobiological Synthesis. In: *Depression.* John Wiley & Sons: New York 1985.
9 Ferguson SM, Brodkin JD, Lloyd GK, Menzaghi F. Antidepressant-like effects of the subtype-selective nicotinic acetylcholine receptor agonist, SIB-1508Y, in the learned helplessness rat model of depression. *Psychopharmacology* 2000; **152**: 295–303.
10 Sherman AD, Petty F. Learned helplessness decreases [^{3}H]imipramine binding in rat cortex. *J Affect Disord* 1984; **6**: 25–32.
11 Mac Sweeney CP, Lesourd M, Gandon JM. Antidepressant-like effects of alnespirone (S 20499) in the learned helplessness test in rats. *Eur J Pharmacol* 1998; **345**: 133–137.
12 Musty RE, Jordan MP, Lenox RH. Criterion for learned helplessness in the rat: a redefinition. *Pharmacol Biochem Behav* 1990; **36**: 739–744.
13 Drevets WC, Price JL, Simpson Jr JR, Todd RD, Reich T, Vannier M *et al.* Subgenual prefrontal cortex abnormalities in mood disorders. *Nature* 1997; **386**: 824–827.
14 Jacobs BL, Praag H, Gage FH. Adult brain neurogenesis and psychiatry: a novel theory of depression. *Mol Psychiatry* 2000; **5**: 262–269.
15 Malberg JE, Eisch AJ, Nestler EJ, Duman RS. Chronic antidepressant treatment increases neurogenesis in adult rat hippocampus. *J Neurosci* 2000; **20**: 9104–9110.
16 Eriksson PS, Perfilieva E, Bjork-Eriksson T, Alborn AM, Nordborg C, Peterson DA *et al.* Neurogenesis in the adult human hippocampus. *Nat Med* 1998; **4**: 1313–1317.
17 Martin P, Soubrie P, Simon P. The effect of monoamine oxidase inhibitors compared with classical tricyclic antidepressants on learned helplessness paradigm. *Progr Neuro-Psychopharmacol Biol Psychiatry* 1987; **11**: 1–7.
18 Nakagawa Y, Ishima T, Ishibashi Y, Tsuji M, Takashima T. Involvement of GABAB receptor systems in action of antidepressants. II: Baclofen attenuates the effect of desipramine whereas muscimol has no effect in learned helplessness paradigm in rats. *Brain Res* 1996; **728**: 225–230.
19 Nakagawa Y, Sasaki A, Takashima T. The GABA(B) receptor antagonist CGP36742 improves learned helplessness in rats. *Eur J Pharmacol* 1999; **381**: 1–7.
20 Tejedor-Real P, Mico JA, Maldonado R, Roques BP, Gibert-Rahola J. Implication of endogenous opioid system in the learned helplessness model of depression. *Pharmacol Biochem Behav* 1995; **52**: 145–152.
21 Anthony JP, Sexton TJ, Neumaier JF. Antidepressant-induced regulation of 5-HT(1b) mRNA in rat dorsal raphe nucleus reverses rapidly after drug discontinuation. *J Neurosci Res* 2000; **61**: 82–87.
22 Bristow LJ, O'Connor D, Watts R, Duxon MS, Hutson PH. Evidence for accelerated desensitisation of 5-HT_{2C} receptors following combined treatment with fluoxetine and the 5-HT_{1A} receptor antagonist, WAY 100,635, in the rat. *Neuropharmacology* 2000; **39**: 1222–1236.
23 Tordera RM, Monge A, Del Rio J, Lasheras B. Antidepressant-like activity of VN2222, a serotonin reuptake inhibitor with high affinity at 5-HT1A receptors. *Eur J Pharmacol* 2002; **442**: 63–71.
24 Mirnics K, Middleton AF, Lewis AD, Levitt P. Analysis of complex brain disorders with gene expression microarrays: schizophrenia as a disease of the synapse. *Trends Neurosci* 2001; **24**: 479–486.
25 Raychaudhuri S, Stuart JM, Altman RB. Principal components analysis to summarize microarray experiments: application to sporulation time series. *Pacific Symp Biocomput* 2000: 455–466.
26 Wurmbach E, Yuen T, Ebersole BJ, Sealfon SC. Gonadotropin-releasing hormone receptor-coupled gene network. *J Biol Chem* 2001; **276**: 47195–47201.
27 Papolos DF, Yu YM, Rosenbaum E, Lachman HM. Modulation of learned helplessness by 5-hydroxytryptamine2A receptor antisense oligodeoxynucleotides. *Psychiatr Res* 1996; **63**: 197–203.
28 Wu J, Kramer GL, Kram M, Steciuk M, Crawford IL, Petty F. Serotonin and learned helplessness: a regional study of 5-HT1A, 5-HT2A receptors

and the serotonin transport site in rat brain. *J Psychiatr Res* 1999; **33**: 17–22.
29 Pandey GN, Pandey SC, Dwivedi Y, Sharma RP, Janicak PG, Davis JM. Platelet serotonin-2A receptors: a potential biological marker for suicidal behavior. *Am J Psychiatry* 1995; **152**: 850–855.
30 Velbinger K, De Vry J, Jentzsch K, Eckert A, Henn F, Muller WE. Acute stress induced modifications of calcium signaling in learned helpless rats. *Pharmacopsychiatry* 2000; **33**: 132–137.
31 Aldenhoff JB, Dumais-Huber C, Fritzsche M, Sulger J, Vollmayr B. Altered Ca(2+)-homeostasis in single T-lymphocytes of depressed patients. *J Psychiatr Res* 1997; **31**: 315–322.
32 Hayaishi O. Molecular mechanisms of sleep–wake regulation: a role of prostaglandin D2. *Philos Trans R Soc London—Ser B Biol Sci* 2000; **355**: 275–280.
33 Mizoguchi A, Eguchi N, Kimura K, Kiyohara Y, Qu WM, Huang ZL *et al.* Dominant localization of prostaglandin D receptors on arachnoid trabecular cells in mouse basal forebrain and their involvement in the regulation of non-rapid eye movement sleep. *Proc Natl Acad Sci USA* 2001; **98**: 11674–11679.
34 Feng J, Cai X, Zhao J, Yan Z. Serotonin receptors modulate GABA(A) receptor channels through activation of anchored protein kinase C in prefrontal cortical neurons. *J Neurosci* 2001; **21**: 6502–6511.
35 Missler M, Hammer RE, Sudhof TC. Neurexophilin binding to alpha-neurexins. A single LNS domain functions as an independently folding ligand-binding unit. *J Biol Chem* 1998; **273**: 34716–34723.
36 Missler M, Sudhof TC. Neurexophilins form a conserved family of neuropeptide-like glycoproteins. *J Neurosci* 1998; **18**: 3630–3638.
37 Nunoue K, Ohashi K, Okano I, Mizuno K. LIMK-1 and LIMK-2, two members of a LIM motif-containing protein kinase family. *Oncogene* 1995; **11**: 701–710.
38 Sarmiere PD, Bamburg JR, Meng Y, Zhang Y, Tregoubov V, Janus C *et al.* Head, neck, and spines. A role for LIMK-1 in the hippocampus. Abnormal spine morphology and enhanced LTP in LIMK-1 knockout mice. *Neuron* 2002; **35**: 3–5.
39 Steffens DC, Krishnan KR. Structural neuroimaging and mood disorders: recent findings, implications for classification, and future directions. *Biol Psychiatry* 1998; **43**: 705–712.
40 Okano I, Hiraoka J, Otera H, Nunoue K, Ohashi K, Iwashita S *et al.* Identification and characterization of a novel family of serine/threonine kinases containing two N-terminal LIM motifs. *J Biol Chem* 1995; **270**: 31321–31330.
41 Altar CA. Neurotrophins and depression. *Trends Pharmacol Sci* 1999; **20**: 59–61.
42 Skolnick P. Antidepressants for the new millennium. *Eur J Pharmacol* 1999; **375**: 31–40.
43 Brandoli C, Sanna A, De Bernardi MA, Follesa P, Brooker G, Mocchetti I. Brain-derived neurotrophic factor and basic fibroblast growth factor downregulate NMDA receptor function in cerebellar granule cells. *J Neurosci* 1998; **18**: 7953–7961.
44 Gould E, Tanapat P. Stress and hippocampal neurogenesis. *Biol Psychiatry* 1999; **46**: 1472–1479.
45 McEwen BS. Stress and hippocampal plasticity. *Annu Rev Neurosci* 1999; **22**: 105–122.
46 McEwen BS. Effects of adverse experiences for brain structure and function. *Biol Psychiatry* 2000; **48**: 721–731.
47 Prince JA, Blennow K, Gottfries CG, Karlsson I, Oreland L. Mitochondrial function is differentially altered in the basal ganglia of chronic schizophrenics. *Neuropsychopharmacology* 1999; **21**: 372–379.
48 Maurer I, Zierz S, Moller H. Evidence for a mitochondrial oxidative phosphorylation defect in brains from patients with schizophrenia. *Schizophr Res* 2001; **48**: 125–136.
49 Jha N, Jurma O, Lalli G, Liu Y, Pettus EH, Greenamyre JT *et al.* Glutathione depletion in PC12 results in selective inhibition of mitochondrial complex I activity. Implications for Parkinson's disease. *J Biol Chem* 2000; **275**: 26096–26101.
50 Chinopoulos C, Adam-Vizi V. Mitochondria deficient in complex I activity are depolarized by hydrogen peroxide in nerve terminals: relevance to Parkinson's disease. *J Neurochem* 2001; **76**: 302–306.
51 Volz HP, Rzanny R, Riehemann S, May S, Hegewald H, Preussler B *et al.* 31P magnetic resonance spectroscopy in the frontal lobe of major depressed patients. *Eur Arch Psychiatr Clin Neurosci* 1998; **248**: 289–295.
52 Jaksch M, Lochmuller H, Schmitt F, Volpel B, Obermaier-Kusser B, Horvath R. A mutation in mt tRNALeu(UUR) causing a neuropsychiatric syndrome with depression and cataract. *Neurology* 2001; **57**: 1930–1931.
53 Kato T. The other, forgotten genome: mitochondrial DNA and mental disorders. *Mol Psychiatry* 2001; **6**: 625–633.
54 Yoshikawa T, Kikuchi M, Saito K, Watanabe A, Yamada K, Shibuya H *et al.* Evidence for association of the myo-inositol monophosphatase 2 (IMPA2) gene with schizophrenia in Japanese samples. *Mol Psychiatry* 2001; **6**: 202–210.
55 Schwab SG, Hallmayer J, Lerer B, Albus M, Borrmann M, Honig S *et al.* Support for a chromosome 18p locus conferring susceptibility to functional psychoses in families with schizophrenia, by association and linkage analysis. *Am J Hum Genet* 1998; **63**: 1139–1152.
56 Kroczka B, Branski P, Palucha A, Pilc A, Nowak G. Antidepressant-like properties of zinc in rodent forced swim test. *Brain Res Bull* 2001; **55**: 297–300.
57 Maes M, Vandoolaeghe E, Neels H, Demedts P, Wauters A, Meltzer HY *et al.* Lower serum zinc in major depression is a sensitive marker of treatment resistance and of the immune/inflammatory response in that illness. *Biol Psychiatry* 1997; **42**: 349–358.
58 Quackenbush J. Computational analysis of microarray data. *Nat Rev Genet* 2001; **2**: 418–427.
59 Steingard RJ, Renshaw PF, Hennen J, Lenox M, Cintron CB, Yuoung AD *et al.* Smaller frontal lobe white matter volumes in depressed adolescents. *Biol Psychiatry* 2002; **52**: 413–417.
60 Cowan WM, Kopnisky KL, Hyman SE. The human genome project and its impact on psychiatry. *Annu Rev Neurosci* 2002; **25**: 1–50.
61 Skolnick P, Legutko B, Li X, Bymaster FP. Current perspectives on the development of non-biogenic amine-based antidepressants. *Pharmacol Res* 2001; **43**: 411–423.
62 Crescenzi M, Giuliani A. The main biological determinants of tumor line taxonomy elucidated by a principal component analysis of microarray data. *FEBS Lett* 2001; **507**: 114–118.
63 Landgrebe J, Welzl G, Metz T, van Gaalen MM, Ropers H, Wurst W *et al.* Molecular characterization of antidepressant effects in the mouse brain using gene expression profiling. *J Psychiatr Res* 2002; **36**: 119–129.

Association of Neural Cell Adhesion Molecule 1 Gene Polymorphisms with Bipolar Affective Disorder in Japanese Individuals

Makoto Arai, Masanari Itokawa, Kazuo Yamada, Tomoko Toyota, Mayumi Arai, Seiichi Haga, Hiroshi Ujike, Ichiro Sora, Kazuhiko Ikeda, and Takeo Yoshikawa

Background: *Although the pathogenesis of mood disorders remains unclear, heritable factors have been shown to be involved. Neural cell adhesion molecule 1 (NCAM1) is known to play important roles in cell migration, neurite growth, axonal guidance, and synaptic plasticity. Disturbance of these neurodevelopmental processes is proposed as one etiology for mood disorder. We therefore undertook genetic analysis of* NCAM1 *in mood disorders.*

Methods: *We determined the complete genomic organization of human* NCAM1 *gene by comparing complementary deoxyribonucleic acid and genomic sequences; mutation screening detected 11 polymorphisms. The genotypic, allelic, and haplotype distributions of these variants were analyzed in unrelated control individuals* (n = *357) and patients with bipolar disorder* (n = *151) and unipolar disorder* (n = *78), all from central Japan.*

Results: *Three single nucleotide polymorphisms, IVS6+32T>C, IVS7+11G>C and IVS12+21C>A, displayed significant associations with bipolar disorder (for allelic associations, nominal* p = *.04,* p = *.02, and* p = *.004, respectively, all* p > *.05 after Bonferroni corrections). Furthermore, the haplotype located in a linkage disequilibrium block was strongly associated with bipolar disorder (the* p *value of the most significant three-marker haplotype is .005).*

Conclusions: *Our results suggest that genetic variations in* NCAM1 *or nearby genes could confer risks associated with bipolar affective disorder in Japanese individuals.*

Key Words: NCAM1, association study, linkage disequilibrium, haplotype, neurodevelopment

Affective disorder is a common psychiatric disease, afflicting approximately 10% of the population worldwide. Once the disease develops, episodes tend to recur throughout life, and prophylaxis is difficult to achieve in some cases with the therapeutic agents currently available. The etiologic bases remain unknown, although twin, family, and adoption studies have provided evidence for the involvement of heritable risk factors (Cardno et al 1999; Craddock and Jones 1999; Mendlewicz and Rainer 1977; Taylor et al 2002). Positive findings from linkage analyses and case–control association studies have also been reported (Berrettini 2000, 2001, 2002; Craddock et al 2001; Kato 2001).

Neural cell adhesion molecule 1 (NCAM1) is a member of the immunoglobulin gene superfamily and is widely expressed in the central nervous system. In addition, three major protein isoforms, of 180 kd, 140 kd, and 120 kd, are well known to possess multiple neurobiological functions in the brain (Kiss and Muller 2001; Ronn et al 1998). The genomic organization has already been partially reported (Saito et al 1994). The 180-kd and 140-kd isoforms of NCAM1 are transmembrane proteins, whereas the 120-kd isoform is linked to the plasma membrane via a glycosyl phosphatidyl-inositol (GPI) lipid anchor. Glycosyl phosphatidyl-inositol is attached to the C-terminal amino acid encoded by exon 15, the exon skipped in the transmembrane forms of NCAM 140 and NCAM 180. The difference between NCAM 140 and NCAM 180 involves the use of exon 18 by the latter isoform (Ronn et al 1998). Furthermore, some alternatively spliced exons exist between exons 7 and 13 (Barton et al 1988; Gower et al 1988; Saito et al 1994; van Duijnhoven et al 1992; also see Figure 1 legend). Several lines of evidence have supported the idea that dysregulation of NCAM1 isoforms in the brain might be involved in the pathophysiology of neuropsychiatric disorders, particularly bipolar affective disorder (Vawter 2000a). Secreted exon (SEC)-NCAM1 is increased in the hippocampus of patients with bipolar disorder (Vawter et al 1999), whereas variable alternative spliced exon (VASE)-NCAM1 is increased in the prefrontal cortex and hippocampus of patients with bipolar disorder (Vawter et al 1998). Furthermore, Poltorak et al (1996) reported elevated concentrations of NCAM1 protein in the cerebrospinal fluid of patients with mood disorder.

In this study, we performed genetic analysis of *NCAM1* as a compelling candidate for involvement in mood disorders.

Methods and Materials

Subjects

Mood disorder samples comprised unrelated patients with bipolar disorder (n = 151; 66% bipolar I, 34% bipolar II) and 78 patients with unipolar disorder (n = 78). Patients with bipolar disorder comprised 80 men (mean age, 49.0 ± 11.9 years) and 71 women (mean age, 48.9 ± 12.4 years). Patients with unipolar disorder comprised 33 men (mean age, 48.1 ± 10.7 years) and 45 women (mean age, 50.7 ± 10.9 years). All patients were diagnosed according to DSM-IV criteria for mood disorder (American Psychiatric Association 1994), to give a best-estimate lifetime diagnosis with consensus from at least two experienced psychi-

From the Department of Schizophrenia Research (MakA, MI, MayA, SH, KI), Tokyo Institute of Psychiatry, Tokyo; Laboratory for Molecular Psychiatry (MI, KY, TT, TY), RIKEN Brain Science Institute, Saitama; Department of Neuropsychiatry (HU), Okayama University Graduate School of Medicine and Dentistry, Okayama; and Department of Neuroscience (IS), Division of Psychobiology, Tohoku University Graduate School of Medicine, Miyagi, Japan.

Address reprint requests to Masanari Itokawa, M.D., Ph.D., Tokyo Institute of Psychiatry, Tokyo Metropolitan Organization for Medical Research, Department of Schizophrenia Research, 2-1-8 Kamikitazawa, Setagaya-ku, Tokyo 156-8585, Japan.

Received August 4, 2003; revised November 20, 2003; accepted January 9, 2004.

0006-3223/04/$30.00
doi:10.1016/j.biopsych.2004.01.009

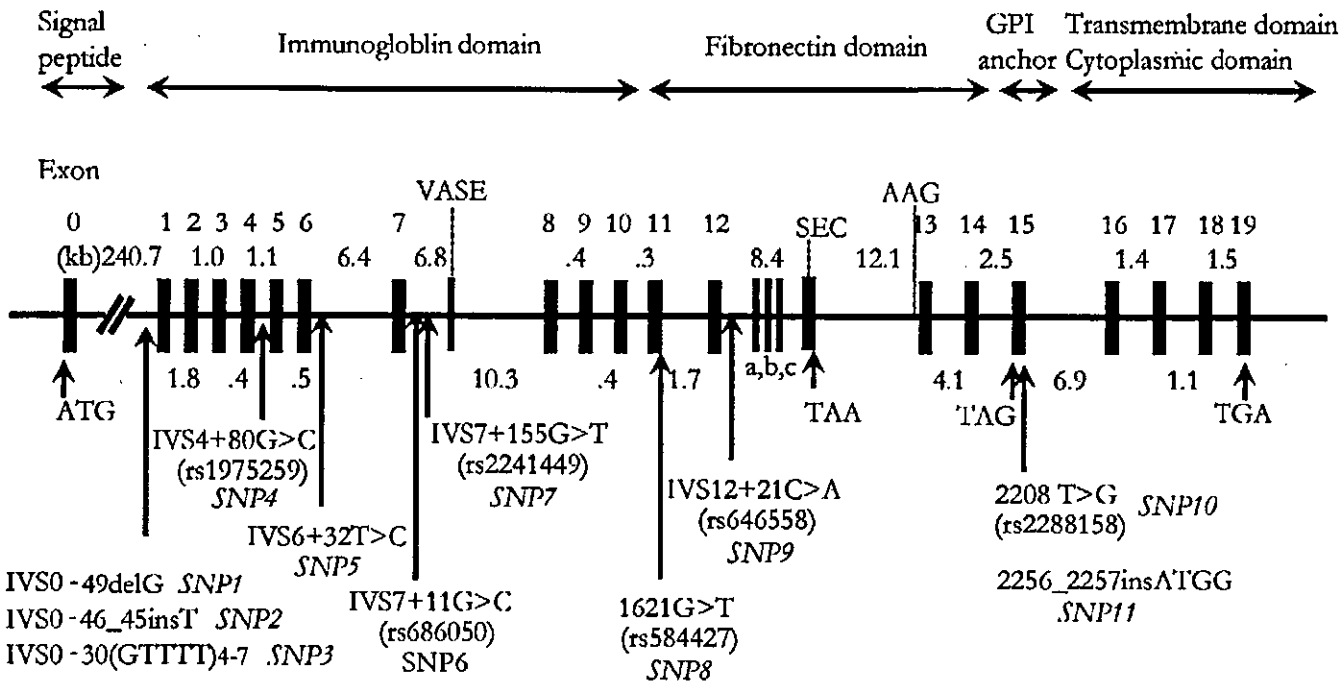

Figure 1. Genomic structure and locations of polymorphic sites for human NCAM1. Exons 0 through 14 are common in all neural cell adhesion molecule (NCAM) isoforms. In addition to the common exons, NCAM 180 uses exons 16, 17, 18, and 19; NCAM 140 uses exons 16, 17, and 19; and NCAM 120 uses exon 15. Locations of the initiation codon (ATG) and stop codons (TAA and TAG), and sizes (kilobases [kb]) of introns are provided. GPI, glycosyl phosphatidylinositol; VASE, variable alternative spliced exon; SEC, secreted exon; a, b, c, and triplet AAG, mini-exons; rs number is the National Center for Biotechnology Information single nucleotide polymorphism (SNP) cluster identification number from the dbSNP database (http://www.ncbi.nlm.nih.gov/SNP/).

atrists. The interview parameters included those described in the Structured Clinical Interview for DSM-IV Axis I Disorders (First et al 1997). All available medical records and family informant reports were also taken into consideration. Control subjects were recruited from among hospital staff and company employees documented to be free from psychoses; they included 173 men (mean age, 50.5 ± 13.5 years) and 184 women (mean age, 52.8 ± 11.0 years). All of our samples were collected from central Japan.

The present study was approved by the Ethics Committees of Tokyo Institute of Psychiatry, RIKEN Brain Science Institute, and Okayama University, and all participants provided written informed consent.

Determination of Genomic Structure

The complete genomic structure of *NCAM1* was determined by comparing complementary deoxyribonucleic acid (DNA) sequence (GenBank accession nos. NM_000615, M22094, S73101, XM_084656, X53243, and AK057509) and the University of California, Santa Cruz (UCSC) April 2003 draft assembly of the human genome (UCSC Genome Bioinformatics web site: http://genome.ucsc.edu/). We newly identified the location of exons VASE (S73101), SEC (M22094), 15 (M22094), 18 (XM_084656, AK057509), and 19 (AK057509). These sequences were not included in the UCSC's gene prediction program. "A" from the ATG initiation codon was considered +1.

Screening for Polymorphisms and Genotyping of Variants

Genomic DNA was isolated from blood samples according to standard methods. All exons and splice boundaries of *NCAM1*, except for some minor exons, were screened for polymorphisms by direct sequencing of polymerase chain reaction (PCR) products, from 20 unrelated bipolar samples. Primers used for PCR amplification are listed in Table 1. Polymerase chain reaction was performed with initial denaturation at 94°C for 1 min, followed by 35 cycles at 94°C for 15 sec, 50°C–70°C (optimized for each primer pair) for 30 sec, 72°C for 45 sec, and final extension at 72°C for 2 min, with TaKaRa Taq polymerase (Takara Bio, Shiga, Japan) or the Expand Long Template PCR System (Roche Diagnotics, Mannheim, Germany). Detailed information on amplification conditions is available upon request. Direct sequencing of PCR products was performed with the BigDye Terminator Cycle Sequencing FS Ready Reaction kit (Applied Biosystems, Foster City, California) and the ABI PRISM 3100 Genetic Analyzer (Applied Biosystems). All the polymorphisms were genotyped by direct sequencing with the help of the SEQUENCHER program (Gene Codes Corporation, Ann Arbor, Michigan), followed by visual inspection by two researchers. When necessary, both strands were sequenced.

Statistical Analysis

Departure from Hardy-Weinberg equilibrium was examined with the χ^2 test. Differences in genotype and allele frequencies were evaluated with Fisher's exact test or the Monte-Carlo method implemented in the CLUMP program (Sham and Curtis 1995) when appropriate. Linkage disequilibrium (LD) statistics were calculated with COCAPHASE (Dudbridge 2002; http://www.hgmp.mrc.ac.uk/~fdudbrid/software/). Estimation and comparison of haplotype frequencies were made with COCAPHASE. Graphic overview of pairwise LD strength between markers was made with GOLD software (Abecasis and Cookson 2000; http://www.well.ox.ac.uk/asthma/GOLD/). Power calculations were performed with Power Calculator (http://calculators.stat.ucla.edu/powercalc/).

Table 1. PCR Primers Used to Search for Nucleotide Variants in the *NCAM1* Gene

Region	Exon Length (bp)	Intron Length (bp)	Primers	Product Size (bp)	3′ End of Primer
Exon 1	75		(F) 5′-AAACTCCACACAAACCTCCTCCC-3′	424	148 bp upstream to exon 1
		1832	(R) 5′-TGCAAAAGGAAGGAAGAGGCCC-3′		159 bp downstream to exon 1
Exon 2	219		(F) 5′-TTCCAGCAGCCATACTCACCCC-3′	498	128 bp upstream to exon 2
		1018	(R) 5′-TTAGGGAGAGAGAATGGGACTG-3′		110 bp downstream to exon 2
Exon 3	144		(F) 5′-TGGAGACTTGCCCAGGACTCA-3′	382	84 bp upstream to exon 3
		376	(R) 5′-AGGACCCAGAAACCACATGAGG-3′		113 bp downstream to exon 3
Exon 4	138		(F) 5′-TCAAAGCCAGGGACGCATTTTC-3′	429	124 bp upstream to exon 4
		1080	(R) 5′-TTACGGTGGGGAGGGGATTTA-3′		126 bp downstream to exon 4
Exon 5	118		(F) 5′-CAATTCCTGACACTAACTCTG-3′	367	124 bp upstream to exon 5
		454	(R) 5′-CCTAAGAAGCCCACATCCATT-3′		85 bp downstream to exon 5
Exon 6	170		(F) 5′-CAGTTGCAGCCCTTGGATAGT-3′	539	182 bp upstream to exon 6
		6366	(R) 5′-ATGATGGTGGCTTGGACTAGG-3′		147 bp downstream to exon 6
Exon 7	143		(F) 5′-ACTAGGGTCTTGTACTTAGCAG-3′	454	94 bp upstream to exon 7
		6784	(R) 5′-TGTGCCTATTCCATTACAAGGG-3′		175 bp downstream to exon 7
VASE	30		(F) 5′-CTAAGGGGGAAAAAAAGCTGGACA-3′	425	181 bp upstream to exon VASE
		10319	(R) 5′-TCATCCACTCCCAACACAGC-3′		173 bp downstream to exon VASE
Exon 8	151		(F) 5′-GATACTCCCAGGTTCTCATGC-3′	583	192 bp upstream to exon 8
		374	(R) 5′-ATGGGAAGAAGACTCAAGGGCA-3′		199 bp downstream to exon 8
Exon 9	185		(F) 5′-TGTTCTGCTTACGTTCCCTGCA-3′	687	256 bp upstream to exon 9
		363	(R) 5′-GAGAAAAGAATAGCAGAGGGGC-3′		204 bp downstream to exon 9
Exon 10	97		(F) 5′-TTGTTTAAGGCTGGGCTGGAG-3′	368	118 bp upstream to exon 10
		332	(R) 5′-AACTCTCTGGCTTTGCTGACC-3′		113 bp downstream to exon 10
Exon 11	171		(F) 5′-ATTGGATCAGCGCATGGGGCA-3′	508	164 bp upstream to exon 11
		1715	(R) 5′-AGGGGCAACAACTCTACAGGCA-3′		132 bp downstream to exon 11
Exon 12	132		(F) 5′-GTCATTTGGGTCTGCCTTTCGG-3′	553	215 bp upstream to exon 12
		8387	(R) 5′-GAAGGGACTGTGTGTTAGCTGTCA-3′		162 bp downstream to exon 12
SEC	239		(F) 5′-GAGGGTGATGCCGAGAAGGAA-3′	661	240 bp upstream to exon SEC
		12086	(R) 5′-CACACGGAGGGAACACCAAGA-3′		142 bp downstream to exon SEC
Exon 13	125		(F) 5′-CTCTCAGTTTGGGCTCAGTC-3′	488	168 bp upstream to exon 13
		4144	(R) 5′-GCTGTAGGGCTGTCTTGGGATT-3′		153 bp downstream to exon 13
Exon 14	178		(F) 5′-GTCCCGTAAGTTTTGCCTATTGTC-3′	434	72 bp upstream to exon 14
		2522	(R) 5′-GCACAGATAGGTACAAGGCAAAAC-3′		138 bp downstream to exon 14
Exon 15	448		(F) 5′-ACCTTCCCTTTCCTTCTGTCCC-3′	746	123 bp upstream to exon 15
		6894	(R) 5′-ATCAGTGCGGTCTGGCTCTTTTAAC-3′		130 bp downstream to exon 15
Exon 16	208		(F) 5′-CTGTTTTCTCAATTCTGGGGCATA-3′	500	148 bp upstream to exon 16
		1364	(R) 5′-CAAATGGAGAACGTGCAATGAAAG-3′		98 bp downstream to exon 16
Exon 17	117		(F) 5′-AAGCTCAAGGTCACACAGCTAG-3′	680	147 bp upstream to exon 17
		1056	(R) 5′-GGTCCCCAGCTTCCCTTATCCTTT-3′		372 bp downstream to exon 17
Exon 18	816		(F) 5′-ATCCTTCTCTCTCTGTGGGCCT-3′	1055	133 bp upstream to exon 18
		1518	(R) 5′-CATCTAACAAGGAGGACACAGCAC-3′		62 bp downstream to exon 18
Exon 19	298		(F) 5′-CTTGGGTGATTTTTAGTGCTCC-3′	1071	146 bp upstream to exon 19
			(R) 5′-GGCAGCTATTTTACACGGACAT-3′		585 bp downstream to exon 19

PCR, polymerase chain reaction; NCAM1, neural cell adhesion molecule 1; F, forward; R, reverse; VASE, variable alternative spliced exon; SEC, secreted exon.

Results

The complete human *NCAM1* spans a region of 314 kilobases (kb) on chromosome 11q23.1, and consists of 19 main exons, exon 0 that encodes the signal peptide, alternatively spliced VASE and SEC exons, and the three-base-pair mini-exon AAG (Figure 1). Two or more alternatively spliced small exons (exons a, b, and c in Figure 1) exist between exons 12 and 13. Although protein isoforms are detected as three major mass classes (180, 140, and 120 kd), combinations of these exons and posttranslational modifications give rise to 20–30 molecular species for NCAM1 (Goridis and Brunet 1992; Kiss and Muller 2001).

Mutation screening allowed us to identify 11 polymorphisms, including five novel variants: IVS0−49delG, IVS0−46_45insT, IVS0−30$(GTTTT)_{4-7}$, IVS6+32T>C, and 2256_2257insATGG (Figure 1). For brevity, the detected single nucleotide polymorphisms (SNPs) were designated as SNP1–11 (Figure 1; Tables 2 and 3). The frequencies (except for that of IVS0−46_45insT, SNP2) are summarized in Tables 2 (SNP3) and 3 (SNPs 1, 4–11). The IVS0−46_45insT genotype could not be accurately determined, owing to the homopolymeric stretch of T nucleotides [$(T)_9$ or $(T)_{10}$]. This polymorphism was thus excluded from subsequent analyses. All polymorphisms were in Hardy-Weinberg equilibrium. Of the 10 polymorphisms, IVS12+21C>A (NCBI dbSNP accession no. rs646558, http://www.ncbi.nlm.nih.gov/SNP/) displayed a nominally significantly different genotypic distribution between patients with bipolar disorder and control subjects (p = .01; Table 3). IVS6+32T>C (novel) and IVS7+11G>C (rs686050) displayed trends toward genotypic association with bipolar disease.